Stress-controlled Poisson ratio of a crystalline membrane: Application to graphene

I. S. Burmistrov,[1,2] I. V. Gornyi,[1,3,4,5] V. Yu. Kachorovskii,[1,3,4,5] M. I. Katsnelson,[6] J. H. Los,[6] and A. D. Mirlin[1,3,5,7]

[1]*L. D. Landau Institute for Theoretical Physics, Kosygina Street 2, 119334 Moscow, Russia*
[2]*Laboratory for Condensed Matter Physics, National Research University Higher School of Economics, 101000 Moscow, Russia*
[3]*Institut für Nanotechnologie, Karlsruhe Institute of Technology, 76021 Karlsruhe, Germany*
[4]*A. F. Ioffe Physico-Technical Institute, 194021 St. Petersburg, Russia*
[5]*Institut für Theorie der kondensierten Materie, Karlsruhe Institute of Technology, 76128 Karlsruhe, Germany*
[6]*Radboud University, Institute for Molecules and Materials, NL-6525AJ Nijmegen, The Netherlands*
[7]*Petersburg Nuclear Physics Institute, 188300 St. Petersburg, Russia*

We demonstrate that a key elastic parameter of a suspended crystalline membrane—the Poisson ratio (PR) ν—is a nontrivial function of the applied stress σ and of the system size L, i.e., $\nu = \nu_L(\sigma)$. We consider a generic two-dimensional membrane embedded into space of dimensionality $2 + d_c$. (The physical situation corresponds to $d_c = 1$.) A particularly important application of our results is to freestanding graphene. We find that at a very low stress, when the membrane exhibits linear response, the PR $\nu_L(0)$ decreases with increasing system size L and saturates for $L \to \infty$ at a value which depends on the boundary conditions and is essentially different from the value $\nu = -1/3$ previously predicted by the membrane theory within a self-consistent scaling analysis. By increasing σ, one drives a sufficiently large membrane (with the length L much larger than the Ginzburg length) into a nonlinear regime characterized by a universal value of PR that depends solely on d_c, in close connection with the critical index η controlling the renormalization of bending rigidity. This universal nonlinear PR acquires its minimum value $\nu_{\min} = -1$ in the limit $d_c \to \infty$, when $\eta \to 0$. With the further increase of σ, the PR changes sign and finally saturates at a positive nonuniversal value prescribed by the conventional elasticity theory. We also show that one should distinguish between the absolute and differential PR (ν and ν^{diff}, respectively). While coinciding in the limits of very low and very high stress, they differ in general: $\nu \neq \nu^{\mathrm{diff}}$. In particular, in the nonlinear universal regime, ν^{diff} takes a universal value which, similarly to the absolute PR, is a function solely of d_c (or, equivalently, of η) but is different from the universal value of ν. In the limit of infinite dimensionality of the embedding space, $d_c \to \infty$ (i.e., $\eta \to 0$), the universal value of ν^{diff} tends to $-1/3$, at variance with the limiting value -1 of ν. Finally, we briefly discuss generalization of these results to a disordered membrane.

I. INTRODUCTION

One of the key elastic parameters of any material is the Poisson ratio (PR)

$$\nu = -\frac{\varepsilon_y}{\varepsilon_x}, \tag{1}$$

which is the coefficient governing the magnitude of transverse deformations ε_y upon longitudinal stretching ε_x. Conventional materials contract in lateral directions when stretched, so that ν is typically positive. However, some exotic, so-called auxetic [1], materials have negative ν. Although some examples of such materials, like a pyrite crystal, were known long time ago [2], the active study of auxeticity started only at the end of 1980s, triggered by the observation of stretching-induced transverse expansion in polyurethane foam [3]. Since then, a negative PR—both in intrinsic materials and in the artificially engineered structures—has been reported in a great number of publications (for recent review see Ref. [4]). The increased interest in auxetic systems is due to their unusual mechanical properties [4], such as increased sound velocity, which is proportional to $(1 + \nu)^{-1/2}$, and enhanced strength.

The purpose of this paper is to explore the PR in graphene, which is a famous two-dimensional (2D) material displaying unique electrical and optical phenomena [5–15]. It also shows unusual elastic properties. In particular, freestanding graphene is a remarkable example of a crystalline 2D membrane with an extremely high bending rigidity $\varkappa \simeq 1$ eV. A distinct feature of such a membrane is the existence of specific types of dynamical and static out-of-plane modes, known as flexural phonons (FPs) [16] and ripples [9,12,13], respectively.

While the PR of graphene-related structures has been the subject of numerous experimental and theoretical works, the results are by far not complete and largely conflicting. The experimental activities have focused on graphene grown on a substrate, with the results for the PR spreading in the range between 0.15 and 0.45 for various substrates (see [17,18] and references therein). These results were apparently influenced by the substrates in an essential way, so that it is difficult to extract from them any information about the PR of a freely standing graphene. A direct measurement of the PR of suspended graphene remains a challenging prospect for future experimental work.

Let us briefly outline the state of the art in the computational analysis of graphene's PR. Early simulations [19] predicted that the PR of pristine graphene (which we term "clean" below as opposed to disordered graphene with impurities and defects)

is positive at ordinary experimental conditions but appears to become negative with the temperature T increasing above a quite large value ($T \gtrsim 1700$ K). Later work [20] supported the conclusion of a positive PR and found its variation with the system size in the interval $0.15 \lesssim \nu \lesssim 0.3$. This value is close to value $\nu \approx 0.17$ found in numerical simulations [21] which did not take into account out-of-plane FP modes.

On the other hand, a number of recent computational studies obtained negative values of the PR for graphene [22–27] and graphene-based engineered structures [28,29], thus demonstrating that graphene does exhibit auxetic properties. In particular, it was found that disorder is highly favorable for auxeticity of the membrane. Specifically, it was reported that introduction of local vacancy defects [22] or artificially designed ripples [23] into a graphene flake leads to negative PR. In a related work, Ref. [24], it was found that the PR is negative in the graphene oxide at a sufficiently large degree of oxidation. Another recent numerical work [26] studied the dependence of PR on the applied stress and came to the conclusion that, while the PR is positive in the limit of zero stress and at very large stresses, it is negative in the intermediate range of stress.

To summarize, the available numerical simulations yield a positive PR of graphene under normal conditions but show that the PR becomes negative at high temperatures [19] or in the presence of sufficiently strong disorder [22–24]. The emergence of an auxetic behavior (negative PR) is qualitatively consistent with expectations based on the membrane theory [30]. Two decades ago, it was found in the framework of this theory that, when the membrane size L exceeds the so-called Ginzburg length L_* [see Eq. (3) below], elastic properties become universal and show an anomalous power-law scaling with L controlled by a critical index η. Recent years witnessed a revival of interest in elastic properties of membranes in the context of graphene and related 2D materials. It was shown, in particular, that anomalous elasticity of graphene leads to anomalous temperature scaling of electric resistivity, formation of large-scale ripples, the nonlinear Hooke's law, and a negative thermal expansion coefficient. These theoretical results are in decent agreement with experimental findings. A more detailed discussion, with references to relevant theoretical and experimental works, is presented in Sec. II.

Within the membrane theory, the PR in the limit of zero stress ($\sigma \to 0$, linear-response regime) was addressed in the framework of the self-consistent screening approximation (SCSA) and predicted [30] to be scale-independent and given by a universal negative value,

$$\nu = -1/3$$

(see also a discussion in Ref. [31] and a review [32]). This result was recently rederived in Ref. [33]. On the numerical side, an early work [34] that performed molecular-dynamics simulations of a membrane with periodic boundary conditions yielded a negative PR, $\nu \approx -0.15$, twice smaller than the analytical value from Ref. [30]. Later simulations, where no boundary constraints were imposed, yielded considerably larger negative values of PR: $\nu \approx -0.32$ for phantom crystalline membranes [35] and $\nu \approx -0.37$ for self-avoiding crystalline membranes [36]. The authors argued that these results are in agreement with the analytical predictions $\nu = -1/3$ of Ref. [30]. While

both Ref. [34], on one side, and Refs. [35,36], on the other side, obtained a negative PR, a clear difference in numerical values calls for an explanation (see also Ref. [37]). If one believes in general applicability of the result $\nu = -1/3$, why did it fail in the case of Ref. [34]? And, if it fails there, under what conditions should it be applicable at all?

The situation becomes even more puzzling if one recalls positive values of PR obtained in numerical simulations for pristine graphene (at room temperature and for lowest values of stress), which should be contrasted to negative values of PR obtained in the earlier membrane simulations. A possible explanation is that the system size in graphene simulations was not sufficiently large. Indeed, it has been recently shown [33] that, with lowering system size, the PR (at $\sigma \to 0$) evolves towards a nonuniversal positive value following from the conventional theory of elasticity. This crossover takes place at system sizes of the order of the Ginzburg length L_*. The value of L_* in graphene at room temperature is 40–70 Å, so that the condition $L > L_*$ appears to be usually satisfied in simulations. Thus, the conclusion that system sizes were not large enough seems somewhat surprising. Did some numerical factors intervene, thus shifting a crossover towards values of L a few times larger than expected? And, finally, why did numerical simulations for disordered graphene show much more pronounced auxetic properties than for clean graphene?

In this paper, we develop a theory of the PR of graphene exemplifying a generic 2D crystalline membrane. Our work extends previous studies in several essential directions. First, we explore the dependence of PR of a finite-size membrane on the applied stress σ. Second, we analyze the difference between the absolute and differential values of PR (ν and ν^{diff}, respectively). We demonstrate that both ν and ν^{diff} are nontrivial functions of the applied uniaxial stress σ and the system size L: $\nu = \nu_L(\sigma), \nu_L^{\mathrm{diff}}(\sigma)$. While coinciding in the limits of very low and very high stresses,

$$\nu_L(0) = \nu_L^{\mathrm{diff}}(0) \quad \text{and} \quad \nu_L(\infty) = \nu_L^{\mathrm{diff}}(\infty),$$

in general, they differ, $\nu \neq \nu^{\mathrm{diff}}$.

We will demonstrate that, for fixed finite L, the PR (both absolute and differential) exhibits, with increasing σ, three distinct regimes (see Fig. 1). In the limit $\sigma \to 0$, the absolute and differential PR coincide and depend on the system size. The "universality" of PR in this regime has a very restricted meaning, even in the limit of large system size ($L \gg L_*$), in contrast to the previous works [30,33] that predicted a truly universal value $-1/3$ of the PR. Specifically, while the linear-response PR of a large membrane is not sensitive to microscopic details of the system, it dramatically depends on the sample shape (aspect ratio) and on boundary conditions (BCs), and can vary by an order of magnitude.

For σ above a small, size-dependent value $\sigma_L \propto 1/L^{2-\eta}$, the system falls into a *universal nonlinear regime* (provided that $L \gg L_*$) where the absolute and differential PRs are close to distinct universal values (the limit $L \to \infty$ is taken first):

$$\nu_\infty(\sigma \to 0) \neq \nu_\infty^{\mathrm{diff}}(\sigma \to 0).$$

The notion of universality here means independence from both microscopic details and BCs. On the other hand, these universal values of ν and ν^{diff} do depend on the dimensionality d_c and,
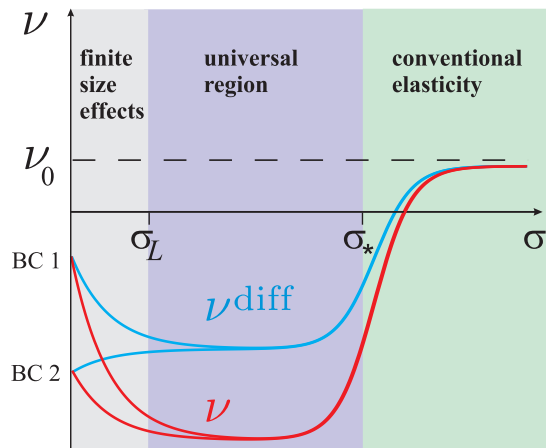
FIG. 1. Schematic dependence of the absolute, $\nu = \nu_L(\sigma)$, and differential, $\nu^{\mathrm{diff}} = \nu_L^{\mathrm{diff}}(\sigma)$, PRs in a crystalline membrane. The characteristic scales of the stress, σ_* and σ_L, are given by Eqs. (24) and (62), respectively. The values of ν and ν^{diff} coincide in the limits of very low and very high stresses, $\nu_L(0) = \nu_L^{\mathrm{diff}}(0)$ and $\nu_L(\infty) = \nu_L^{\mathrm{diff}}(\infty)$. At $\sigma \ll \sigma_L$, the PR is negative and depends on boundary conditions as indicated by curves BC 1 and BC 2 corresponding to the different boundary conditions. At $\sigma \gg \sigma_*$, the PR is positive and is given by the (material-dependent) value ν_0 prescribed by the conventional elasticity theory. In the universal nonlinear regime, $\sigma_L \ll \sigma \ll \sigma_*$, the absolute and differential PRs have different negative universal values ν_∞ and $\nu_\infty^{\mathrm{diff}}$ which depend solely on the dimensionality $2 + d_c$ of the embedding space, i.e., on the critical index η. For $d_c \to \infty$ (i.e., $\eta \to 0$) these universal values exhibit the limiting behavior $\nu_\infty \to -1$ and $\nu_\infty^{\mathrm{diff}} \to -1/3$, respectively.

in general, none of them is equal to $-1/3$, as discussed below. With the further increase of σ, the absolute and differential PRs change sign and finally saturate at the positive nonuniversal value ν_0 prescribed by the conventional elasticity theory.

Importantly, we show that the PR depends on the critical index η (which is, in turn, a function of the dimensionality $d = 2 + d_c$ of the embedding space) controlling the renormalization of bending rigidity and playing a key role in the crumpling and buckling transitions that can occur in a crystalline membrane (see discussion in Sec. II). An analytical calculation of the PR for a physical 2D membrane in a three-dimensional space ($d_c = 1$) thus encounters a severe obstacle: the absence of a small parameter that would control the analysis. To overcome this difficulty, we consider the limit of large d_c, where $\eta \simeq 2/d_c$ can be treated as a small parameter. We demonstrate that a small value of η allows one to controllably calculate both the absolute and differential PR. In particular, in the universal nonlinear regime, $\sigma_L < \sigma < \sigma_*$ [for definitions of σ_L and σ_* see Eqs. (24) and (62) below], we find

$$\nu \to -1 \quad \text{and} \quad \nu^{\mathrm{diff}} \to -1/3$$

in the limit of large dimensionality $d_c \to \infty$ (i.e., $\eta \to 0$). Leading corrections to these values are linear in η. We also find analytically the values of $\nu_L^{\mathrm{diff}}(0) = \nu_L(0)$ for various boundary conditions in the $\eta \to 0$ limit.

For a physical membrane with $d_c \sim 1$, the value of η is not at all small, $\eta \approx 0.7$–0.8. Thus, the values of PR in all the above

regimes will differ substantially from the corresponding values at $d_c \to \infty$ (or, equivalently, $\eta \to 0$). On the other hand, all the basic physical features of the functions $\nu_L(\sigma)$ and $\nu^{\mathrm{diff}}(\sigma)$ are expected to be the same at $d_c = 1$ and at large d_c. Furthermore, we find a relatively small value of the numerical coefficient in front of the linear-in-η term in the expansion for ν^{diff}. This suggests that the values of PR found in this work may serve as reasonable approximations for a physical membrane in a three-dimensional space.

We also discuss briefly the opposite limit, $\eta \to 1$, which is formally realized at $d_c \to 0$ [30]. In this limit, effects of anomalous elasticity get suppressed with decreasing d_c, coming into play only at exponentially large scales, $L > \tilde{L}_*$, where $\ln \tilde{L}_* \propto 1/d_c$. (The definition of $\tilde{L}_*$ is given in Sec. IV B.) For $L < \tilde{L}_*$, both the absolute and differential PRs remain close to ν_0.

Finally, we consider the PR of a disordered membrane. The physics is largely analogous in this case; however, the universality class is different. In particular, the index of anomalous elasticity has a distinct value, $\eta_{\mathrm{dis}} \simeq \eta/4$. As a result, the disordered membrane in the physical dimensionality ($d_c = 1$) is much closer to the $d_c \to \infty$ (or, equivalently, $\eta \to 0$) limit than the clean one, which implies that disorder favors auxetic properties. We also show that in the linear-response ($\sigma \to 0$) regime the PR of a disordered membrane exhibits strong mesoscopic fluctuations.

II. ANOMALOUS ELASTICITY OF A GENERIC MEMBRANE

We start with recalling basic notions of the anomalous elasticity of a generic crystalline membrane. One of the remarkable phenomena that may occur in such a membrane is the crumpling transition (CT), i.e., a transition between the flat and crumpled phases. The problem of crumpling has a close relation to the well known problem of thermodynamic stability of 2D crystals [38,39] (see Refs. [12,13] for a more recent discussion).

The underlying physics is the competition between thermal fluctuations and strong anharmonic coupling between in-plane vibration modes and FPs [16]. In contrast to the in-plane phonons with the linear dispersion, the FPs are very soft, $\omega_{\mathbf{q}} \propto q^2$. Consequently, the out-of-plane thermal fluctuations are unusually strong and tend to destroy the membrane by driving it into the crumpled phase [16]. The competing effect is the anharmonicity that suppresses thermal fluctuations and, therefore, plays here a key role. This question was intensively discussed more than two decades ago [16,30,40–55] in connection with biological membranes, polymerized layers, and inorganic surfaces. The interest to this topic has been renewed more recently [56–64] after discovery of graphene. It was found [40–46] that the anharmonic coupling of in-plane and out-of-plane phonons stabilizes the membrane for not too high temperatures T. This class of problems is under active investigation now since measurement of the elasticity of freestanding graphene is accessible to current experimental techniques [65–69]. An additional interest to this topic is due to the significant effect of the FPs and ripples on electrical and thermal conductivities of graphene (see Refs. [70,71] and references therein).

The CT temperature $T_{\rm cr}$ is proportional to the bending rigidity [72,73] and, consequently, is very high for graphene (on the order of several eV). Because of the high value of $\varkappa$, *clean* graphene remains flat up to all realistic temperatures, $T \lesssim \varkappa$, and the CT cannot be directly observed. Remarkably, a crystalline membrane is predicted to show a critical behavior even very far from the CT transition point, deep in the flat phase. This is connected with a strong renormalization of the bending rigidity [30,45,47], $\varkappa \to \varkappa_q$, for sufficiently small wave vectors $q \ll q_*$ according to the RG equation [30,45,47],

$$d\varkappa/d\Lambda = \eta\varkappa \;\; \Rightarrow \;\; \varkappa_q = \varkappa_0 (q_*/q)^\eta. \tag{2}$$

Here $\Lambda = \ln(q_*/q)$, η is the anomalous dimension of the bending rigidity (critical index of CT), q_* is the inverse Ginzburg length,

$$q_* = \frac{1}{L_*} \simeq \sqrt{d_c\,\tilde{\mu}\,T}/\varkappa_0, \tag{3}$$

$\tilde{\mu} = 3\mu_0(\mu_0 + \lambda_0)/[8\pi(2\mu_0 + \lambda_0)]$ (see, e.g., Ref. [72]), μ_0, λ_0 are the bare in-plane elastic constants (Lamé coefficients), and $\varkappa_0$ the bare bending rigidity. The critical exponent η was determined within several approximate analytical schemes [30,43,45,46,57]; none of them is controllable in the physical case of a 2D membrane embedded in the three-dimensional space. Numerical simulations for latter case yield $\eta = 0.60 \pm 0.10$ [51], $\eta = 0.72 \pm 0.04$ [55], and $\eta = 0.85$ [56].

As a consequence of strong anharmonicity, key characteristics of graphene, such as the conductivity at the Dirac point [70] and elastic moduli [72], show a nontrivial power-law scaling with the system size and temperature. Physically, this scaling manifests the tendency of the membrane to the flat phase with increasing system size for temperatures below the crumpling transition temperature. [The latter condition is always satisfied for a graphene membrane; see Eq. (18) below.] One of the most important consequences is that the linear Hooke's law fails even in the limit of an infinitesimally small tension [20,33,44,46,47,69,73]. Specifically, the deformation ΔL of a membrane subjected to a small stretching tension $\sigma > 0$ scales as $\Delta L \propto \sigma^\alpha$, with a nontrivial exponent α which is expressed in terms of the critical index η as

$$\alpha = \frac{\eta}{2 - \eta}. \tag{4}$$

In the opposite case, $\sigma < 0$, $\Delta L < 0$, the membrane undergoes a buckling transition [44], with α being the critical index of this transition. Another remarkable manifestation of the anomalous elasticity characterized by the critical scaling in the flat phase is that the thermal expansion coefficient of graphene is negative and depends on η [74].

Influence of static disorder on membrane elasticity has been discussed since early works [49,50,53]. In recent years, this question has attracted a great deal of attention in connection with ripples—*static* out-of-plane deformations induced by disorder. In particular, in a recent paper by three of the authors [72], a theory of rippling and crumpling in *disordered* freestanding graphene was developed. The coupled RG equations describing the combined flow of the bending rigidity and disorder strength were derived and rippling in the flat phase was explored. It was shown that the static disorder can strongly affect elastic properties of the membrane. In

particular, the corresponding scaling exponent turns out to be four times smaller than in the clean case, $\eta_{\rm dis} \simeq \eta/4$. It was also demonstrated [73] that, similarly to the clean case, the linear Hooke's law in *disordered* graphene breaks down at low stresses. Importantly, both in the clean and disordered cases, α is expressed in a simple way via the critical index η but the values of α for clean and disordered graphene are different and given by $\alpha(\eta)$ and $\alpha(\eta_{\rm dis})$, respectively.

These findings imply that FPs and ripples can be studied on equal footing. For weak disorder, FPs dominate, while at sufficiently strong disorder the anomalous elasticity of graphene is fully determined by the static random ripples. The nonlinearity of elasticity of graphene found in Ref. [73] is in agreement with recent experimental findings [68,69]. Related theoretical results have been recently obtained for clean membranes in the ribbon geometry [33].

In this work, we mainly focus on the study of the PR of clean graphene. However, based on the similarity of the problems of FPs and ripples, we supplement this analysis by a discussion of the disordered case.

III. BALANCE EQUATIONS FOR MEMBRANE

In this section, we extend the theory of nonlinear elasticity of 2D membranes [73] to study the PR. For the sake of generality, we consider (following earlier studies of membranes) a more general case of a membrane with dimension $D = 2$ embedded in the d-dimensional space with $d = 2 + d_c > 2$. The physical situation corresponds to $d = 3$.

The starting point of our analysis is the energy functional

$$E = \int d^2x \left[\frac{\varkappa_0}{2}(\Delta\mathbf{r})^2 + \frac{\mu_0}{4}(\partial_\alpha\mathbf{r}\partial_\beta\mathbf{r} - \delta_{\alpha\beta})^2 \right.$$
$$\left. + \frac{\lambda_0}{8}(\partial_\gamma\mathbf{r}\partial_\gamma\mathbf{r} - D)^2 \right], \tag{5}$$

where $\varkappa_0$ is the bare bending rigidity, while μ_0 and λ_0 are the in-plane coupling constants. The d-dimensional vector $\mathbf{r} = \mathbf{r}(\mathbf{x})$ describes a point on the membrane surface and depends on the 2D coordinate $\mathbf{x} = x\mathbf{e}_x + y\mathbf{e}_y$ that parametrizes the membrane. Here, $\mathbf{e}_x$ and $\mathbf{e}_y$ are the unit vectors in the reference plane. The vector $\mathbf{r}$ can be split into

$$\mathbf{r} = \xi_{ij}x_i\mathbf{e}_j + \mathbf{u} + \mathbf{h}, \tag{6}$$

where vectors $\mathbf{u} = (u_x, u_y)$, $\mathbf{h} = (h_1, \ldots, h_{d_c})$ represent in-plane and out-of-plane displacements, respectively. Homogeneous stretching of the membrane in the x and y directions is described by the tensor ξ_{ij}. For isotropic deformations $\xi_{ij} = \xi\delta_{ij}$. In the absence of external tension, within the mean-field approximation, the stretching factor ξ equals unity. Fluctuations (in particular, out-of-plane deformations) lead to a decrease of ξ, so that at finite T the stretching factor becomes smaller than unity.

Here, we consider the reaction of the membrane to external forces applied in the x and y directions. For simplicity, we do not discuss shear deformations. We thus assume that ξ_{ij} has two nonzero spatially independent components:

$$\xi_{xx} = \xi_x, \;\; \xi_{yy} = \xi_y. \tag{7}$$

Details of the derivation of the free energy F are relegated to Appendix, where we obtain Eq. (49) for F as a function of global deformations ξ_x and ξ_y. One can find the balance equation by differentiating F with respect to deformations, $\sigma_\alpha = L^{-2}\partial F/\partial\xi_\alpha$, where σ_α are components of the external stress applied to the membrane. As a result, we get

$$\sigma_\alpha = M_{\alpha\beta}\frac{\xi_\beta^2 - 1 + K_\beta}{2}, \qquad (8)$$

where

$$K_\alpha = \left\langle K_\alpha^0 \right\rangle = \int \frac{d\mathbf{x}}{L^2}\langle(\partial_\alpha\mathbf{h})^2\rangle, \quad \alpha = (x,y), \qquad (9)$$

are the bulk-averaged anomalous deformations K_α^0 [see Eq. (A2)], also averaged over the Gibbs distribution with the energy functional Eq. (5) under the fixed value of the external tension. The matrix of elastic constants reads

$$\hat{M} = \begin{pmatrix} 2\mu_0 + \lambda_0 & \lambda_0 \\ \lambda_0 & 2\mu_0 + \lambda_0 \end{pmatrix}. \qquad (10)$$

Unusual anomalous properties of membranes which are not captured by the conventional elasticity theory are connected with the shrinking of the effective area of the membrane (projected area) caused by the transverse fluctuations [75]. The effect of transverse fluctuations is described by the anomalous deformations K_α which are (by definition) some functions of global deformations ξ_x and ξ_y, and, consequently [via Eqs. (8)], of the stress: $K_\alpha = K_\alpha(\sigma_x, \sigma_y)$. The anomalous deformations can be expressed in terms of the correlation function $G_\mathbf{q}$ of FPs:

$$K_\alpha = d_c \int \frac{d^2\mathbf{q}}{(2\pi)^2}q_\alpha^2 G_\mathbf{q}, \qquad (11)$$

where $G_\mathbf{q}$ is defined as

$$\langle h_{\alpha,\mathbf{q}}h_{\beta,-\mathbf{q}}\rangle = \delta_{\alpha\beta}G_\mathbf{q}. \qquad (12)$$

Within the harmonic approximation, the bending rigidity is given by its bare value and the correlation function reads:

$$G_\mathbf{q}^{\text{har}} = \frac{T}{\varkappa_0 q^4 + \sum_\alpha \sigma_\alpha q_\alpha^2}. \qquad (13)$$

The term $\sum_\alpha \sigma_\alpha q_\alpha^2$ in the denominator accounts for a finite stress applied to the membrane. The anharmonic coupling between FPs and in-plane modes leads to essential modification of the correlation function (13). In particular, the account of this coupling within the random phase approximation (RPA) scheme leads to a replacement of the bare value $\varkappa_0$ with the renormalized scale-dependent bending rigidity, $\varkappa_q$, in the denominator of Eq. (13) [see Eq. (58) below].

Equations (8) are the basis for our further study. For the sake of generality, we also present in Appendix the balance equations and expressions for elastic moduli for a membrane of dimensionality $D \neq 2$.

The dependence of the anomalous deformations K_α on the applied stress is the key point for further consideration. Let us split K_α into two parts,

$$K_\alpha(\sigma_x, \sigma_y) = K(0) - \delta K_\alpha(\sigma_x, \sigma_y), \qquad (14)$$

where

$$K(0) = K_x(0,0) = K_y(0,0) \qquad (15)$$

is the anomalous deformation at zero stress. Physically, the deformation $K(0)$ arises because of the shrinking of the membrane in the longitudinal direction caused by temperature-induced transverse fluctuations. In a clean membrane, this deformation is proportional to the temperature [46,72,73], $K(0) = T/T_{\text{cr}}$, and can be fully incorporated in the renormalization of ξ_α in the unstressed membrane:

$$\xi_\alpha^2 - 1 \longrightarrow \xi_\alpha^2 - \xi_0^2, \qquad (16)$$

where

$$\xi_0^2 = 1 - K(0) = 1 - \frac{T}{T_{\text{cr}}} \qquad (17)$$

and T_{cr} is the critical temperature for the crumpling.

We will assume that the membrane is in the flat phase far from the CT,

$$T \ll T_{\text{cr}} \propto \varkappa. \qquad (18)$$

For graphene, where $\varkappa \approx 1$ eV, this is the case at all realistic temperatures. Then,

$$\xi_0 \approx 1$$

and

$$\xi_\alpha^2 - \xi_0^2 \approx 2\varepsilon_\alpha,$$

where

$$\varepsilon_\alpha = \xi_\alpha - \xi_0$$

is a small deformation. Equation (8) then yields

$$\varepsilon_x = \frac{\sigma_x - \nu_0\sigma_y}{Y_0} + \frac{\delta K_x(\sigma_x,\sigma_y)}{2}, \qquad (19)$$

$$\varepsilon_y = \frac{\sigma_y - \nu_0\sigma_x}{Y_0} + \frac{\delta K_y(\sigma_x,\sigma_y)}{2}, \qquad (20)$$

where

$$Y_0 = \frac{4\mu_0(\mu_0 + \lambda_0)}{2\mu_0 + \lambda_0}, \quad \nu_0 = \frac{\lambda_0}{2\mu_0 + \lambda_0} \qquad (21)$$

are the bare values of the Young modulus and of the PR, respectively.

Equations (19) and (20) represent the general balance equations for a crystalline membrane (in the absence of shear deformations) deep in the flat phase. The key new ingredients of these equations, compared to balance equations of the conventional elasticity theory, are anomalous deformations δK_α. Physically, the anomalous deformations at finite σ account for uncrumpling, i.e., "ironing" of the membrane by the external stress. We will start with a phenomenological approach to anomalous elasticity by considering $\delta K_\alpha(\sigma_x,\sigma_y)$ to be a given function of σ_x and σ_y. The analytical expressions for these deformations will be presented later [see Eq. (77)].

We proceed now by briefly reminding the reader of implications of the anomalous elasticity in the case of an isotropic stress and then by giving a general definition of the absolute and differential PR. We will assume here the limit of a large system size, $L \to \infty$, taken at a given value of stress. Finite-size effects will be analyzed in Sec. V.

A. Isotropic deformation

Of central importance for anomalous elasticity is a strong renormalization of the elastic constants by anomalous deformations δK_α. To explain this point, we first note that for isotropic deformations $\sigma_x = \sigma_y = \sigma$, $\varepsilon_x = \varepsilon_y = \varepsilon$, $\delta K_x = \delta K_y = \delta K(\sigma)$. The balance equations then reduce to the following equation relating σ and ε:

$$\varepsilon = \frac{\sigma}{k_0} + \frac{\delta K(\sigma)}{2}, \tag{22}$$

in agreement with Refs. [46,73]. Here, $k_0 = 2(\mu_0 + \lambda_0) \sim \mu_0$ is the bare in-plane stiffness. (Here and below, we assume in all order-of-magnitude estimates that the bare elastic constants have the same order of magnitude: $\lambda_0 \sim \mu_0 \sim Y_0 \sim k_0$.) As shown in Ref. [73], the renormalized stiffness $k_{\rm eff} = \partial\sigma/\partial\varepsilon$ coincides with k_0 for large σ but is suppressed in a power-law way,

$$k_{\rm eff} \sim k_0 \left(\frac{\sigma}{\sigma_*}\right)^{1-\alpha}, \tag{23}$$

for $\sigma < \sigma_*$, where

$$\sigma_* \simeq \varkappa_0 q_*^2 \simeq \frac{\mu_0 T}{\varkappa}, \tag{24}$$

and α is a critical index of buckling transition, which can be expressed in terms of η according to Eq. (4). For $\sigma \ll \sigma_*$, the deformation ϵ is fully determined by the anomalous contribution: $\varepsilon \simeq \delta K(\sigma)/2$. The anomalous Hooke's law (23) originates from the critical scaling of the bending rigidity, Eq. (2).

B. Absolute Poisson ratio

Let us now consider a membrane subjected to an uniaxial stress in the x direction:

$$\sigma_x = \sigma, \quad \sigma_y = 0. \tag{25}$$

The balance equations become

$$\varepsilon_x = \frac{\sigma}{Y_0} + \frac{\delta K_x(\sigma,0)}{2}, \tag{26}$$

$$\varepsilon_y = -\frac{\nu_0\sigma}{Y_0} + \frac{\delta K_y(\sigma,0)}{2}. \tag{27}$$

Resolving these equations, we find the Young modulus and the absolute PR:

$$Y = \frac{\sigma}{\varepsilon_x} = \frac{Y_0}{1 + Y_0\delta K_x/2\sigma}, \tag{28}$$

$$\nu = -\frac{\varepsilon_y}{\varepsilon_x} = \frac{\nu_0 - Y_0\delta K_y/2\sigma}{1 + Y_0\delta K_x/2\sigma}. \tag{29}$$

(Here and below we omit arguments of δK_α for the sake of compactness.) One can easily check that the Young modulus and the absolute PR are connected by conventional expressions [see Eqs. (21)] with the effective Lamé coefficients λ and μ found from the equations

$$\mu = \frac{\mu_0}{1 + \mu_0\delta K_-/\sigma}, \tag{30}$$

$$\mu + \lambda = \frac{\mu_0 + \lambda_0}{1 + 2(\mu_0 + \lambda_0)\delta K_+/\sigma}, \tag{31}$$

where

$$\delta K_+ = \frac{\delta K_x + \delta K_y}{2}, \quad \delta K_- = \delta K_x - \delta K_y. \tag{32}$$

In order to clarify the physical meaning of $\delta K_\pm$, we notice that the matrix $M_{\alpha\beta}$ defined by Eq. (10) is diagonalized by the transformation from σ_x, σ_y to $\sigma_\pm = \sigma_x \pm \sigma_y$. Physically, this means that within the conventional elasticity there are two types of deformations: (i) isotropic deformations with $\epsilon_x = \epsilon_y$ and (ii) deformations with $\epsilon_x = -\epsilon_y$, which correspond to eigenvalues $2(\mu_0 + \lambda_0)$ and $2\mu_0$ of the matrix $\hat{M}$, respectively. Equations (30) and (31) show how these eigenvalues are modified by the anomalous deformations.

The absolute PR is expressed in terms of $\delta K_\pm$ as follows:

$$\frac{\nu + 1/3}{Y} = \frac{\nu_0 + 1/3}{Y_0} + \frac{\delta K_- - \delta K_+}{3\sigma}. \tag{33}$$

In the limit of large anomalous deformations, $\delta K_\alpha/\sigma \gg 1/Y_0$, we find $Y \simeq 2\sigma/\delta K_x$ and

$$\lambda = -\frac{\mu}{2}\left(1 + \frac{\delta K_+ - \delta K_-}{\delta K_+}\right), \tag{34}$$

$$\nu = -\frac{\delta K_y}{\delta K_x} = -\frac{1}{3} + \frac{4}{3}\frac{\delta K_- - \delta K_+}{2\delta K_+ + \delta K_-}. \tag{35}$$

We see that the Lamé coefficients belong to the so-called invariant manifold [30], $\lambda = -\mu/2$, and the absolute PR equals $-1/3$ only provided that $\delta K_- = \delta K_+$. However, as we demonstrate below, the latter equation is not satisfied even in the limit $d_c \to \infty$.

C. Differential Poisson ratio

Next we consider the response of a membrane with respect to small variations $\delta\sigma_x$ and $\delta\sigma_y$. Substituting $\sigma_x = \sigma_x^0 + \delta\sigma_x$ and $\sigma_y = \sigma_y^0 + \delta\sigma_y$ into Eqs. (19) and (20), we find the linear-in-$\delta\sigma_\alpha$ variations of deformations

$$\delta\varepsilon_x = \frac{\delta\sigma_x - \nu^{\rm diff}\delta\sigma_y}{Y^{\rm diff}}, \tag{36}$$

$$\delta\varepsilon_y = \frac{\delta\sigma_y - \nu^{\rm diff}\delta\sigma_x}{Y^{\rm diff}}. \tag{37}$$

Here

$$Y^{\rm diff} = \frac{Y_0}{1 + Y_0\Pi_{xx}/2T}, \tag{38}$$

$$\nu^{\rm diff} = \frac{\nu_0 - Y_0\Pi_{xy}/2T}{1 + Y_0\Pi_{xx}/2T} \tag{39}$$

are the "differential" values of the Young modulus and the PR, respectively, and

$$\Pi_{\alpha\beta} = -T\frac{\partial K_\beta(\sigma_x^0, \sigma_y^0)}{\partial\sigma_\alpha^0} = T\frac{\partial\delta K_\beta(\sigma_x^0, \sigma_y^0)}{\partial\sigma_\alpha^0} \tag{40}$$

are the zero-momentum components of the polarization operator $\Pi_{\alpha\beta\gamma\delta}^{\mathbf{q}}$ (which is a rank-four tensor) [30,47,72],

$$\Pi_{xx} = \Pi_{xxxx}^{\mathbf{q}\to 0}, \quad \Pi_{xy} = \Pi_{xxyy}^{\mathbf{q}\to 0}. \tag{41}$$

The values of the differential Young modulus and PR are connected by conventional relations of the form (21) with the

screened values of the Lamé coefficients, μ^{diff} and λ^{diff}, which can be found from

$$\mu^{\text{diff}} = \frac{\mu_0}{1 + \mu_0 \Pi_- / T}, \tag{42}$$

$$\mu^{\text{diff}} + \lambda^{\text{diff}} = \frac{\mu_0 + \lambda_0}{1 + 2(\mu_0 + \lambda_0)\Pi_+ / T}, \tag{43}$$

where

$$\Pi_+ = \frac{\Pi_{xx} + \Pi_{xy}}{2}, \quad \Pi_- = \Pi_{xx} - \Pi_{xy}. \tag{44}$$

The physical sense of $\Pi_\pm$ is analogous to that of $\delta K_\pm$ discussed below Eq. (32). Equations (42) describe the "differential screening" of the two eigenvalues of the matrix $\hat{M}$.

One can express the differential PR in terms of $\Pi_\pm$ in a way similar to Eq. (33):

$$\frac{\nu^{\text{diff}} + 1/3}{Y^{\text{diff}}} = \frac{\nu_0 + 1/3}{Y_0} + \frac{\Pi_- - \Pi_+}{3T}. \tag{45}$$

In the limit of strong screening, $\Pi_{\alpha\beta} \gg 1/Y_0$, we find $Y^{\text{diff}} \simeq 2T/\Pi_{xx}$ and

$$\lambda^{\text{diff}} = -\frac{\mu_{\text{diff}}}{2}\left(1 + \frac{\Pi_+ - \Pi_-}{\Pi_+}\right), \tag{46}$$

$$\nu^{\text{diff}} = -\frac{\Pi_{xy}}{\Pi_{xx}} = -\frac{1}{3} + \frac{4}{3}\frac{\Pi_- - \Pi_+}{2\Pi_+ + \Pi_-}. \tag{47}$$

For $\Pi_- = \Pi_+$, the Lamé coefficients belong to the invariant manifold, $\lambda^{\text{diff}} = -\mu^{\text{diff}}/2$, and the PR equals $-1/3$. As we will show below, this happens only in the limit $d_c \to \infty$.

The differential Young modulus and the differential PR, as well as the polarization tensor, are functions of the initial stress (σ_x^0, σ_y^0). In the rest of the paper, when discussing the differential PR, we assume an isotropic case, $\sigma_x^0 = \sigma_y^0 = \sigma$, i.e., $Y^{\text{diff}} = Y^{\text{diff}}(\sigma, \sigma)$, $\nu^{\text{diff}} = \nu^{\text{diff}}(\sigma, \sigma)$ and $\Pi_{xx} = \Pi_{xx}(\sigma, \sigma)$, $\Pi_{xy} = \Pi_{xy}(\sigma, \sigma)$. It is worth noticing that Eqs. (38) and (39) for the differential response in the case of an isotropic stress σ can be obtained from Eqs. (28) and (29) for the absolute response to an uniaxial stress σ by the replacement

$$\frac{\delta K_x(\sigma, 0)}{\sigma} \to \frac{\Pi_{xx}(\sigma, \sigma)}{T}, \quad \frac{\delta K_y(\sigma, 0)}{\sigma} \to \frac{\Pi_{xy}(\sigma, \sigma)}{T}. \tag{48}$$

IV. CALCULATION OF POISSON RATIO

As a first step of calculation of the PR, one can integrate out the in-plane modes in the energy functional (5), thus arriving (in the absence of the external tension) at a functional

$$\frac{E[\mathbf{h}]}{T} = \frac{\varkappa}{2T}\int (dk)k^4 |\mathbf{h_k}|^2 + \frac{1}{8}\int (dk\,dk'dq)R_{\mathbf{q}}(\mathbf{k}, \mathbf{k}')$$
$$\times (\mathbf{h_{k+q}}\mathbf{h_{-k}})(\mathbf{h_{-k'-q}}\mathbf{h_{k'}}), \tag{49}$$

which depends on $\mathbf{h}$ fields only [30]. Here, we use a shorthand notation $(dk) = d^2\mathbf{k}/(2\pi)^2$. The anharmonic interaction between $\mathbf{h}$ and $\mathbf{u}$ fields is encoded in $E[\mathbf{h}]$ in the $\mathbf{h}^4$ interaction term with the coupling

$$R_{\mathbf{q}}(\mathbf{k}, \mathbf{k}') = Y_0 \frac{[\mathbf{k} \times \mathbf{q}]^2}{q^2}\frac{[\mathbf{k}' \times \mathbf{q}]^2}{q^2}. \tag{50}$$

Hence, the bare Young modulus serves as a bare coupling constant. The bare propagator (which is exact in the absence of interaction, $R = 0$) is given by Eq. (13).

The interaction coupling constants get screened in analogy with conventional charges in a media with a finite polarizability. Within the RPA, one replaces Y_0 with

$$Y_{\mathbf{q}} = \frac{Y_0}{1 + Y_0 \Pi_{xxxx}^{\mathbf{q}} / T} \tag{51}$$

in Eq. (50), so that the screened coupling constant is $\mathbf{q}$-dependent. For large systems, $L \gg L_*$, the properties of the membrane are determined by the infrared universal region, $q \ll 1/L_*$, where interaction is proportional to the inverse polarization operator [30] (see also Ref. [72]):

$$Y_{\mathbf{q}} = T / \Pi_{xxxx}^{\mathbf{q}}. \tag{52}$$

We note that the bare coupling Y_0 drops out from the expression (52) for the interaction in this regime.

The next step is to study the nonlinear $\mathbf{h}^4$ model with the screened interaction (52). In the absence of the external tension, the correlation functions of $\mathbf{h}$ fields scales as follows [16]:

$$G_{\mathbf{q}}(\sigma = 0) = \frac{T}{\varkappa_q q^4} \propto \frac{1}{q^{4-\eta}}. \tag{53}$$

Equation (53) differs from Eq. (13) with $\sigma = 0$ by a replacement of the bare value of the bending rigidity $\varkappa_0$ with the value $\varkappa_q$ that scales with q in a power-law way [see Eq. (2)]. The components of the polarization operator scale then as follows [30,47]:

$$\Pi_{\alpha\beta\gamma\theta}(\sigma = 0) \propto d_c \left(\frac{T}{q\varkappa_q}\right)^2 \propto \frac{1}{q^{2-2\eta}}, \tag{54}$$

while the interaction constant scales in the universal region as

$$Y_{\mathbf{q}}(\sigma = 0) = \frac{q^2 \varkappa_q^2}{d_c T} \propto q^{2-2\eta}. \tag{55}$$

The critical scaling of the bending rigidity can be obtained within the SCSA scheme [30] by self-consistently solving the coupled equations for the self-energy and the RPA screened interaction with the simplest polarization bubbles included; see Fig. 2. Within the SCSA, the critical exponent η for a 2D membrane embedded into the space of dimensionality $2 + d_c$
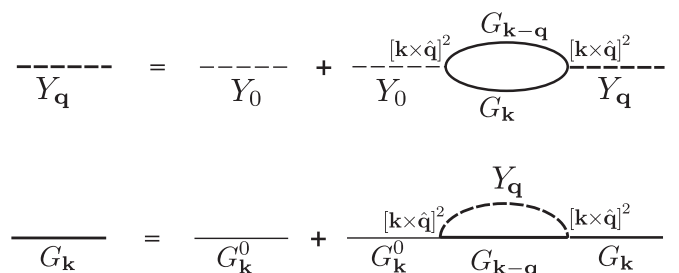
FIG. 2. Self-consistent screening approximation: Graphical representation of the SCSA equations for the screened interaction $Y_{\mathbf{q}}$ and the propagator $G_{\mathbf{k}}$. The bare Green's function $G_{\mathbf{k}}^0$ is given by Eq. (13). Vertices are given by $[\mathbf{k} \times \hat{\mathbf{q}}]^2$, where $\hat{q} = \mathbf{q}/q$.

FIG. 3. Diagram for function K_α. The thick line denotes the propagator $G_\mathbf{k}$ at finite tension. For calculating the terms in PR of zeroth and first orders in $1/d_c$, it is sufficient to use $G_\mathbf{k}$ defined in Fig. 2.

is given by [30]

$$
\eta = \frac{4}{d_c + \sqrt{16 - 2d_c + d_c^2}}
$$
$$
\rightarrow \begin{cases} \frac{2}{d_c} + \frac{1}{d_c^2}, & \text{for} \quad d_c \rightarrow \infty, \\ 1 - \frac{3d_c}{16}, & \text{for} \quad d_c \rightarrow 0. \end{cases} \tag{56}
$$

Actually, only the asymptotics at $d_c \rightarrow \infty$ is controlled by the small parameter $1/d_c$. For an arbitrary d_c (in particular, for the physical case $d_c = 1$), there is no small parameter controlling the SCSA calculations. Therefore, in the limit of large d_c, the SCSA calculation yields correctly only the leading term $2/d_c$ in η, while an evaluation of higher-order corrections requires going beyond the SCSA.

The situation with the calculation of the PR is quite similar. In this case, in order to find the absolute and differential PR, one should calculate functions K_α and $\Pi_{\alpha\beta}$ (which is found from a more general polarization operator $\Pi_{\alpha\beta\gamma\theta}$), respectively. There are two nontrivial problems here: the inclusion of the external tension (in the nonlinear regime) and an accurate account of finite-size effects (in the linear-response regime). As we are going to discuss below, these complications do not allow one to find exact numerical values of ν and ν^{diff}, as this would require a resummation of all orders in $1/d_c$. Therefore, in what follows we will calculate the PR analytically only for $d_c \gg 1$ making use of the small parameter $\eta \ll 1$.

In order to calculate the terms in PR of zeroth and first orders in $1/d_c$ it is sufficient to evaluate the simplest diagram for K_α in Fig. 3 with the propagators $G_\mathbf{q}$ defined in Fig. 2. This is similar to finding the leading-in-$1/d_c$ term in η within the SCSA. The corrections to the PR coming from diagrams that are not included in the set given by Figs. 2 and 3 are quadratic in $1/d_c$. Importantly, despite $\eta \ll 1$, the elastic coefficients are strongly renormalized at large L and small σ. Thus, the evaluation of the PR at $d_c \gg 1$ does not assume the lowest-order perturbation theory and requires a resummation of an infinite series of diagrams in terms of bare propagators (13).

Let us start with scaling estimates. To this end, we take into account the tension by introducing the term with the external tension into the denominator of Eq. (53):

$$
G_\mathbf{q} = \frac{T}{\varkappa_q q^4 + \sigma_x q_x^2 + \sigma_y q_y^2}, \tag{57}
$$

which amounts to the replacement $\varkappa_0 \rightarrow \varkappa_q$ in Eq. (13). This gives the Green's functions

$$
G_\mathbf{q} = \frac{T}{\varkappa_q q^4 + \sigma q_x^2} \quad \text{and} \quad \mathcal{G}_\mathbf{q} = \frac{T}{\varkappa_q q^4 + \sigma q^2} \tag{58}
$$

for the calculation of the absolute and differential PRs, respectively. These functions correctly describe the asymptotics of

the true Green's functions in limits of both large and small q. Specifically, they coincide with Eq. (53) for $q \gg \tilde{q}_\sigma$, where [73]

$$
\tilde{q}_\sigma \simeq q_* \left(\frac{\sigma}{\sigma_*} \right)^{1/(2-\eta)} \tag{59}
$$

is found from the condition $\varkappa_q q^2 \simeq \sigma$ and σ_* is given by Eq. (24). For $q \ll \tilde{q}_\sigma$, the tension terms in the denominators of the Green's functions dominate and one can neglect the term $\varkappa_q q^4$. It is worth emphasizing that the appearance of external tension σ in the denominator of the Green's function of membrane with anharmonic coupling is a consequence of the corresponding Ward identity [46,47,76]. The approximation (58) corresponds to the neglect of the tension σ in the self-energy of the propagator $G_\mathbf{q}$. The status of this approximation will be discussed below.

The integrals entering δK_α and $\Pi_{\alpha\beta}$ are determined by $q \sim \tilde{q}_\sigma$. Importantly, for $\sigma \ll \sigma_*$, the characteristic scale $\tilde{q}_\sigma$ goes beyond the inverse Ginzburg length $\tilde{q}_\sigma \ll q_*$, so that the membrane falls into the universal regime (see Fig. 1). In particular, in the interval $\tilde{q}_\sigma \ll q \ll q_*$, the components of the polarization operator obey the universal power-law scaling (54) and saturate at a value $\sim (T/\tilde{q}_\sigma \varkappa_{\tilde{q}_\sigma})^2$ for $q \sim \tilde{q}_\sigma$. Hence,

$$
\Pi_{\alpha\beta} \sim \left(\frac{T}{q \varkappa_q} \right)^2_{q \simeq \tilde{q}_\sigma} \sim \frac{T}{\mu} \left(\frac{\sigma_*}{\sigma} \right)^{1-\alpha}, \tag{60}
$$

where α is given by Eq. (4). Analogously, estimating δK_α from the diagram shown in Fig. 3, one finds

$$
\frac{\mu \delta K_\alpha}{\sigma} \sim \left(\frac{\sigma_*}{\sigma} \right)^{1-\alpha}. \tag{61}
$$

As follows from Eqs. (60) and (61), for $\sigma \ll \sigma_*$ both absolute and differential PRs are fully determined by anomalous deformations and, therefore, universal. They are given by Eqs. (47) and (35), respectively. Hence, the membrane exhibits universal elastic properties for $\sigma \ll \sigma_*$.

There is also a lower bound on σ for a membrane to show this universal PR. Indeed, we assumed above that the membrane has infinite size. For a finite square-shaped membrane with $L_* \ll L < \infty$, one can neglect finite-size effects provided that $\tilde{q}_\sigma \gg 1/L$. The latter inequality yields $\sigma \gg \sigma_L$, where

$$
\sigma_L \sim \sigma_* \left(\frac{L_*}{L} \right)^{2-\eta} \ll \sigma_*. \tag{62}
$$

In the opposite limit, $\sigma \ll \sigma_L$, one can neglect tension terms in the denominator of $G_\mathbf{q}$ and $\mathcal{G}_\mathbf{q}$ [see Eq. (58)] in the whole interval of $q \gtrsim 1/L$. Then, the membrane shows linear response with respect to the external tension and

$$
\nu = \nu^{\text{diff}}, \quad \text{for} \quad \sigma \ll \sigma_L. \tag{63}
$$

A naive approach to the analysis of finite-size effects is to introduce the infrared cutoff $q \simeq 1/L$ into the integrals determining δK_α and $\Pi_{\alpha\beta}$. The PR in this regime still shows a certain universality, in the sense that it does not depend on microscopic details of the models. However, as we discuss in detail in Sec. V, it is strongly sensitive to the BCs which determine the system behavior at the scale $q \sim 1/L$. As a result, depending on BCs, the PR at $\sigma = 0$ can be either larger

or smaller than its value in the universal regime, $\sigma_L < \sigma < \sigma_*$; see Fig. 1.

We return now to the regime of nonlinear universality, $\sigma_L \ll \sigma \ll \sigma_*$, and emphasize the following important point. Although the approach described above captures correctly the scaling properties of the problem, it does not allow for the calculation of exact numerical values of ν and ν^{diff}. Indeed, for calculation of the PR one needs to know the exact behavior of the Green's functions with the σ-dependent self-energy $\Sigma(\mathbf{q}; \sigma_x, \sigma_y)$,

$$G_{\mathbf{q}} = \frac{T}{\varkappa_0 q^4 + \sigma_x q_x^2 + \sigma_y q_y^2 - \Sigma(\mathbf{q}; \sigma_x, \sigma_y)}$$
$$\simeq \frac{T}{\varkappa_q q^4 + \sigma_x q_x^2 + \sigma_y q_y^2 - \delta\Sigma(\mathbf{q}; \sigma_x, \sigma_y)}, \quad (64)$$

in the crossover region $q \simeq \tilde{q}_\sigma$ [here $\delta\Sigma(\mathbf{q}; \sigma_x, \sigma_y) = \Sigma(\mathbf{q}; \sigma_x, \sigma_y) - \Sigma(\mathbf{q}; 0, 0)$ is the stress-induced correction to the self-energy]. In a generic situation (i.e., for $\eta \sim 1$), this behavior is complex and not known even within the SCSA as defined in Fig. 2. In particular, equations (58) for $G_{\mathbf{q}}$ and $\mathcal{G}_{\mathbf{q}}$ are only approximate (up to a $\mathbf{q}$-dependent factor of order unity) in the crossover region. The approximation becomes controllable only in the limit of $\eta \ll 1$. The point is that for small η the bending rigidity grows very slowly and does not change essentially when q varies by a factor on the order of 2. Hence, in the leading order, one can use for calculations of PR the functions (58) with the replacement of the scale-dependent $\varkappa_q$ with $\varkappa_{\tilde{q}_\sigma}$. However, already linear-in-η corrections to the PR are sensitive to the dependence of the self-energy on σ and on the angle of $\mathbf{q}$. This dependence was neglected within the approximation (58) (which can be termed "zero-σ SCSA") by setting $\delta\Sigma(\mathbf{q}; \sigma_x, \sigma_y) = 0$. It is worth noticing that, even at small η, the bending rigidity at $q \simeq \tilde{q}_\sigma$ can be much larger than $\varkappa_0$ provided that the tension is sufficiently weak, $\ln(\sigma_*/\sigma) \gtrsim 1/\eta$. The values of ν and ν^{diff} in the small-η (i.e., large-d_c) limit will be discussed in Sec. IV A.

A. Small η

For large dimensionality d_c the calculation of the PR is controlled by a small parameter η. This allows us to develop a systematic expansion in η. We demonstrate this below by considering the differential and absolute PRs.

1. Differential PR

Let us consider the diagrams in Fig. 4 for the polarization operator. In the leading-in-$1/d_c$ approximation, the tensor $\Pi_{\alpha\beta\gamma\delta}^{\mathbf{q}}$ is given by the diagram without vertex corrections shown in Fig. 4(a), where thick lines correspond to isotropic (in q space) functions $\mathcal{G}_{\mathbf{q}}$ [see Eq. (58)]. Within this approximation, the polarization tensor is fully isotropic in the limit $q \to 0$:

$$\Pi_{\alpha\beta\gamma\delta}^{\mathbf{q}\to 0} = C(\delta_{\alpha\beta}\delta_{\gamma\theta} + \delta_{\alpha\gamma}\delta_{\beta\theta} + \delta_{\alpha\theta}\delta_{\beta\gamma}), \quad (65)$$

where

$$C = \frac{d_c}{3} \lim_{q \to 0} \int_0^\infty k_\perp^4 \mathcal{G}_{\mathbf{k}} \mathcal{G}_{\mathbf{k}-\mathbf{q}} \frac{d^2 k}{(2\pi)^2}. \quad (66)$$

Here $\mathcal{G}_{\mathbf{k}}$ is given by Eq. (58) and $k_\perp^4 = |\mathbf{k} \times \mathbf{q}/q|^4$. (This definition of the polarization operator differs by a numerical
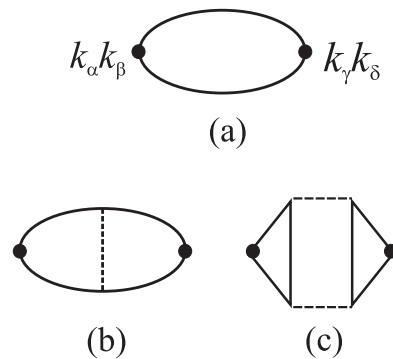
FIG. 4. Diagrams for polarization operator $\Pi_{\alpha\beta\gamma\theta}$ used for the calculation of the differential PR at $d_c \gg 1$. Thick lines denote the renormalized propagator $G_{\mathbf{k}}$ and dashed lines denote the renormalized interaction $Y_{\mathbf{q}}$ as defined in Fig. 2. Diagram (a) yields the leading term in the differential PR, while diagrams (b) and (c) provide the $1/d_c$ correction. Diagram (c) has the same order as (b), since the smallness $1/d_c$ from the extra dashed line is compensated by the factor d_c coming from the extra loop. By virtue of Eq. (40), the vertex-correction diagrams (b) and (c) are obtained by differentiating the *self-energy* of the propagator $G_{\mathbf{q}}$ in Fig. 3 with respect to σ_α and hence cannot be generated within the approximation (58).

coefficient from the one used in Ref. [72].) Hence, within this $d_c \to \infty$ approximation

$$\Pi_{xx} = 3\Pi_{xy} = 3C, \quad (67)$$

$$\Pi_+ = \Pi_- = 2C. \quad (68)$$

Substituting this in Eq. (47), we obtain $\nu^{\text{diff}} = -1/3$, which is exactly the result of Ref. [30]. It is worth noting that this number can be obtained in a straightforward way without actual calculation of the integral over k in Eq. (66). Indeed, in the absence of vertex corrections, $\Pi_{xx} \propto \langle n_x^4 \rangle$ and $\Pi_{xy} \propto \langle n_x^2 n_y^2 \rangle$, with the same coefficient. Here $\mathbf{n} = \mathbf{k}/k$ and $\langle \cdots \rangle$ stands for the angle averaging. Then, we get $\langle n_x^4 \rangle = 3/8$ and $\langle n_x^2 n_y^2 \rangle = 1/8$, and finally obtain

$$\nu^{\text{diff}} = -\frac{\langle n_x^2 n_y^2 \rangle}{\langle n_x^4 \rangle} = -\frac{1}{3}. \quad (69)$$

Importantly, this result is not valid when vertex corrections are included in the polarization bubble, such as in Figs. 4(b) and 4(c). A general structure of the polarization operator is [47]

$$\Pi_{\alpha\beta,\gamma\theta}^{\mathbf{q}\to 0} = C_1 \delta_{\alpha\beta}\delta_{\gamma\theta} + C_2(\delta_{\alpha\gamma}\delta_{\beta\theta} + \delta_{\alpha\theta}\delta_{\beta\gamma}), \quad (70)$$

with $C_1 \neq C_2$. Hence, in the general case,

$$\Pi_{xx} = C_1 + 2C_2, \qquad \Pi_{xy} = C_1. \quad (71)$$

A direct analysis of diagrams Figs. 4(b) and 4(c) shows that the condition $C_1 = C_2$ indeed fails when the vertex corrections are included. Consequently, conditions $\Pi_{xx} = 3\Pi_{xy}$ and $\Pi_+ = \Pi_-$ also fail. In a general case, $\Pi_{xx} - 3\Pi_{xy} = 2(C_2 - C_1)$. Hence, in a generic membrane with $\eta \sim 1$ the differential PR is not equal to $-1/3$. This applies, in particular, to physical membranes in a three-dimensional space, in which case $d_c = 1$ and $\eta \approx 0.7$–0.8.

Let us discuss this point in more detail. A scaling analysis of the diagrams in Fig. 4 shows that for $q_\sigma \ll q \ll q_*$ the components of the polarization operator increase with decreasing q as $1/q^{2-2\eta}$:

$$\Pi_{xxxx} = C_{xx}\frac{T^2}{(q\varkappa_q)^2}, \quad \Pi_{xxyy} = C_{xy}\frac{T^2}{(q\varkappa_q)^2}, \quad (72)$$

where C_{xx} and C_{xy} are numerical coefficients. The PR is given in terms of these coefficients as

$$\nu^{\text{diff}} = -\frac{C_{xy}}{C_{xx}}. \quad (73)$$

To the leading order (zeroth order in η), the PR is determined by the diagram of Fig. 4(a), yielding $\nu^{\text{diff}} = -1/3$, as discussed above. Corrections of the first order in η come from the diagrams 4(b) and 4(c). Indeed, each interaction line gives a factor $1/d_c \sim \eta$, see Eq. (55), so that the diagram 4(b) yields a correction of order η. The diagram 4(c), although of second order in interaction, contains an additional polarization loop that gives a factor $d_c \sim 1/\eta$, and thus contributes to the order η along with the diagram 4(b).

The calculation of the numerical coefficient resulting from the diagrams 4(b) and 4(c) is lengthy and will be presented elsewhere [76]. The result reads

$$\nu^{\text{diff}} = -\tfrac{1}{3} + 0.008\eta + O(\eta^2). \quad (74)$$

The correction proportional to η is due to a difference between the polarization operators Π_+ and Π_-, which emerges in the order η:

$$\frac{\Pi_+ - \Pi_-}{\Pi_+} \simeq 0.018\eta. \quad (75)$$

Thus, the exact value of ν^{diff} is a universal function of η which can be obtained in a controllable way by an expansion over powers of η. The value $-1/3$ is obtained only in the limit $\eta \to 0$, i.e., at $d_c \to \infty$. For a finite d_c, vertex corrections lead to appearance of a nonzero value of $(\Pi_+ - \Pi_-)/\Pi_+$ which is absent in the lowest order and yields corrections to ν^{diff}.

2. Absolute PR

Let us now consider the absolute PR. Within the approximation (58), the anomalous deformation reads

$$K_\beta(\sigma,0) = d_c T \int \frac{d^2q}{(2\pi)^2} \frac{q_\beta^2}{\varkappa_q q^4 + \sigma_\varphi q^2}$$
$$= K(0) - \delta K_\beta(\sigma,0). \quad (76)$$

All stress dependence is encoded in the function

$$\delta K_\beta(\sigma,0) = \frac{d_c T}{2\pi}\left\langle \int_0^\infty \frac{dq}{q} \frac{n_\beta^2 \sigma_\varphi}{\varkappa_q(\varkappa_q q^2 + \sigma_\varphi)} \right\rangle_\varphi. \quad (77)$$

Here

$$\sigma_\varphi = \sigma\cos^2\varphi, \quad (78)$$

and $\langle\cdots\rangle_\varphi$ stands for averaging over φ. It is worth emphasizing that in contrast to ν^{diff}, which represents a linear response to a small anisotropic stress on top of a large isotropic one, the absolute PR describes an essentially nonlinear response. This is clearly reflected in Eq. (77), where the applied stress σ_φ

enters both the numerator and the denominator. The integral (77) is determined by momenta $q \sim \tilde{q}_\sigma$. For $\sigma \ll \sigma_*$ such q are located in the region of the anomalous elasticity $q \ll q_*$, where the renormalized bending rigidity $\varkappa_q$ scales with q in a power-law way. As a result, δK_β turn out to be power-law functions of σ. For $\sigma \gg \sigma_*$, the bending rigidity $\varkappa_q$ is approximately given by its bare value $\varkappa$, so that δK_β grows as $\ln\sigma$. Thus, we get from Eq. (77)

$$\frac{Y_0 \delta K_\beta}{2\sigma} = \begin{cases} A_0(\sigma_*/\sigma)^{1-\alpha}\langle n_x^{2\alpha} n_\beta^2\rangle_\varphi, & \text{for } \sigma \ll \sigma_*, \\ A_1(\sigma_*/\sigma)\ln(\sigma_*/\sigma), & \text{for } \sigma \gg \sigma_*, \end{cases} \quad (79)$$

where A_0 and A_1 are numerical coefficients of order unity and α is given by Eq. (4). (We remind the reader that in all estimates we assume that all bare elastic constants are of the same order and absorb the corresponding dimensionless ratios in prefactors of order unity.)

It is seen from Eqs. (29) and (79) that for $\sigma \gg \sigma_*$ the Young modulus and the PR are given, to the leading order, by their bare values. On the other hand, for $\sigma \ll \sigma_*$ anomalous terms dominate and we find

$$Y \sim Y_0(\sigma/\sigma_*)^{1-\alpha} \quad (80)$$

and the following result for the PR,

$$\nu = \nu_{\min} = -\frac{\langle \cos^{2\alpha}\varphi \sin^2\varphi \rangle_\varphi}{\langle \cos^{2\alpha+2}\varphi \rangle_\varphi} = -\frac{1}{1+2\alpha}$$
$$= -\frac{2-\eta}{2+\eta}. \quad (81)$$

Hence, the Young modulus Y is suppressed due to the softening of the membrane by thermal fluctuations, while ν equals a certain universal value, $\nu_{\min}$, which is determined solely by the critical index η (i.e., by the dimensionality d_c). In full analogy with the differential PR, the result (81) for the absolute PR is strictly valid only at $\eta = 0$, yielding in this limit $\nu_{\min} = -1$. For a generic $\eta \sim 1$ (and, in particular, for the physically relevant case $d_c = 1$) it constitutes an uncontrollable approximation. In order to find a correction of the first order in η, one should take into account, in addition to the correction $\sim\eta$ entering Eq. (81), the deviation of the propagator $G_{\mathbf{q}}$ from its approximate form (58). The difference stems from the dependence of the self-energy on σ. The resulting expansion of ν up to the first-order term in η reads

$$\nu_{\min} = -1 + (1 + C_\Sigma)\eta + O(\eta^2), \quad (82)$$

where C_Σ is the contribution to the coefficient of the η correction resulting from the stress dependence of self-energy. The evaluation of the numerical coefficient C_Σ is very tedious and is postponed to a forthcoming publication. Importantly, for an anisotropic tension, the exact self-energy in Eq. (64) depends on the angle of $\mathbf{q}$, so that the effect of anharmonic interaction at $q \simeq \tilde{q}_\sigma$ is not fully captured by the $|q|$-dependent function $\varkappa_q$.

Substituting Eq. (79) into Eq. (29), one can find the subleading correction to Eq. (81):

$$\nu_{\min}(\sigma) \approx \nu_{\min} + A_2(\sigma/\sigma_*)^{1-\alpha}, \quad \text{for } \sigma_L \ll \sigma \ll \sigma_*, \quad (83)$$

where $A_2 \sim 1$ is a positive numerical coefficient. The lower boundary σ_L of the region of validity of Eq. (83) is determined by the system size L [see Eq. (62)] providing the infrared cutoff

to Eq. (77). In the limit of an infinite system, $L = \infty$, we have $\sigma_L = 0$, so that Eq. (83) is applicable down to arbitrarily weak stresses.

Two comments are in order before closing this subsection. First, comparing Eq. (82) with Eq. (35), we see that $\delta K_+ \neq \delta K_-$ even in the limit $\eta \to 0$. As seen from Eq. (79), this happens because in this limit (which implies also $\alpha \to 0$), $\delta K_\beta \propto \langle n_\beta^2 \rangle$. Hence, anomalous deformations in the x and y directions coincide: $\delta K_x = \delta K_y$ and, consequently, $\delta K_- \equiv 0$ [see Eq. (32)] for $\eta = 0$. Then we find from Eq. (35) $\nu \to -1$, in agreement with Eq. (82).

The second comment concerns the generalization of the above results obtained under condition of the uniaxial stress ($\sigma_x = \sigma, \sigma_y = 0$) to the case of more general deformations. This should be done with caution. In particular, the uniaxial modulus C_{11}—which is one of the most conventional characteristics of an elastic media—is ill defined for a membrane with negative PR. Indeed, by definition, C_{11} corresponds to $\varepsilon_y = 0$. The latter condition prevents expansion in the y direction and therefore should lead to a transverse wrinkling instability. A detailed study of this instability is an interesting prospect for future work.

B. $\eta \to 1$

As we have shown above, the large-d_c limit (which corresponds to small η) allows one to get a controllable approximation (and, in principle, also an expansion in powers of $\eta \sim 1/d_c$) for the PR. It is natural to ask whether the opposite limit of small d_c can be used to develop a complementary approximation. The limiting value $d_c = 0$ corresponds to a 2D membrane embedded into 2D space. Evidently, because of the absence of out-of-plane modes, the anomalous deformations, which are proportional to the number of transverse modes, are exactly equal to zero in this limit, $K_\beta \propto d_c = 0$ for $d_c = 0$. Hence, in-plane moduli are not renormalized by anomalous elasticity in this limit, so that the membrane should obey the conventional Hooke's law [Eqs. (19) and (20) with $\delta K_\beta = 0$]. This corresponds to the index $\alpha = 1$, and thus, according to Eq. (4), $\eta = 1$. In this situation, both the absolute and differential PRs are equal to the nonuniversal material value ν_0:

$$\nu = \nu^{\text{diff}} = \nu_0 \quad \text{for} \quad \eta = 1. \tag{84}$$

Let us now turn to the range of small but nonzero dimensionality d_c. In this case, η is not exactly equal to unity but is close to it, $1 - \eta \sim d_c \ll 1$. The polarization operator then behaves logarithmically,

$$\Pi_{\alpha\beta\gamma\theta} \propto d_c \frac{T}{\mu} \ln\left(\frac{q_*}{q}\right), \tag{85}$$

in an exponentially wide interval of q:

$$\tilde{q}_* < q < q_*, \tag{86}$$

where

$$\tilde{q}_* \sim q_* \exp(-1/d_c) \tag{87}$$

is inversely proportional to the spatial scale $\tilde{L}_*$ at which the anomalous elasticity becomes fully developed: $\tilde{L}_* \sim 1/\tilde{q}_*$. Within the interval (86), the anomalous deformations can be

treated perturbatively, so that PR (both absolute and differential) remains close to ν_0. Only for exponentially small wave vectors, $q \ll \tilde{q}_*$ (or, equivalently, for exponentially large size, $L \gg \tilde{L}_*$), the membrane falls into the universal regime, so that anomalous deformations scale in a power-law way with q. In particular, the polarization operator then scales in accordance with Eq. (72). The differential PR takes a universal value which can be determined from Eq. (73).

Unfortunately, at this stage, we are not able to present a controllable scheme for the evaluation of this universal value of ν^{diff} for small d_c. The result $\nu^{\text{diff}} = -1/3$ given by the diagram of Fig. 4(a) is strongly modified by higher-order corrections. The only essential simplification is the smallness of diagrams containing more then one full-line loop, such as the diagram shown in Fig. 4(c). Such diagrams can be neglected, since each loop gives an additional small factor d_c. On the other hand, one can check that all high-order diagrams containing a single full-line loop do not have any additional small factors $\sim d_c$ and, therefore, should be taken into account along with the diagram in Fig. 4(a). The evaluation of the numerical value of ν^{diff} in this regime thus requires a summation of an infinite set of diagrams, which remains a challenging problem for future research. A similar conclusion holds for the absolute PR for $q \ll \tilde{q}_*$. Via the same token, one can check that the value of the coefficient in the first order of the expansion of the exponent η over d_c is modified in an uncontrollable way by higher-order terms as compared to the value $-3/16$ in the lower line of Eq. (56) (cf. a discussion in Ref. [58]).

To summarize, we find that for small d_c (i.e., η close to unity) both the absolute and differential PR remain close to the nonuniversal material parameter ν_0 within the broad interval of system sizes determined by Eq. (86) but eventually flow to still unknown values for the exponentially large systems, $L \gg 1/\tilde{q}_*$.

V. FINITE-SIZE EFFECTS

In this section, we analyze the effect of a finite size of a membrane on the PR. Consider, for example, the absolute PR. Within the approximation (58), the finite size L of the system determines the infrared cutoff in the integral in Eqs. (77). As a result, Eqs. (80) and (81) become invalid at low stress $\sigma < \sigma_L$, where σ_L is given by Eq. (62). Let us consider a square-shaped sample with the size $L \gg L_*$ and assume that the membrane is stretched by small tensions:

$$\sigma_x \ll \sigma_L, \quad \sigma_y \ll \sigma_L. \tag{88}$$

We will demonstrate that in this case the value of the PR strongly depends on the boundary conditions. This should be taken into account when one compares results of analytical, numerical, and experimental evaluation of PR. The importance of the BCs for numerical simulations of the PR was recently pointed out in Ref. [26].

A. Poisson ratio

In the regime that we are considering, thermodynamic fluctuations of the strain are relatively strong, as will be

discussed below. The PR is defined as

$$\nu = -\frac{\langle \varepsilon_y \rangle}{\langle \varepsilon_x \rangle}, \quad \nu^{\text{diff}} = -\frac{\langle \delta \varepsilon_y \rangle}{\langle \delta \varepsilon_x \rangle}, \tag{89}$$

where $\langle \ldots \rangle$ denotes the thermodynamic averaging. This definition corresponds to the diagrammatic approach described in the previous sections.

For a finite system, the integration in Eq. (77) for the anomalous deformations should be replaced with the summation. Minimal q entering the sum is limited by $\sim 1/L$. Then, one can neglect $\sigma_\varphi = \sigma_x \cos^2 \varphi + \sigma_y \sin^2 \varphi$ in the denominator of the integrand. As a consequence, δK_β becomes a linear function of σ_x and σ_y and the absolute and differential responses coincide:

$$\nu = \nu^{\text{diff}} \quad \text{for} \quad \sigma \ll \sigma_L, \tag{90}$$

which is a manifestation of the fact that we are in the linear-response regime with respect to the external stress. For a not too small system, $L \gg L_*$, anomalous deformations dominate over the conventional ones, and $\varepsilon_\beta \simeq \delta K_\beta / 2$. The scaling of δK_β can be understood within the approximation (58) (one can check that high-order corrections do not change this scaling).

Assuming a symmetry between the x and y axes (which implies a square shape of the sample), one can write the balance equations, which have the form analogous to Eqs. (36) and (37),

$$\varepsilon_x \simeq \frac{1}{Y_L}(\sigma_x - \nu \sigma_y), \tag{91}$$

$$\varepsilon_y \simeq \frac{1}{Y_L}(-\nu \sigma_x + \sigma_y), \tag{92}$$

with the size-dependent Young modulus

$$Y_L \simeq Y_0 \left(\frac{L_*}{L} \right)^{2-2\eta}. \tag{93}$$

In Eq. (93) we have used the fact that in the considered regime the system size L provides the infrared cutoff for the anomalous scaling of the elastic modulus. Equations (91) and (92) represent the general form of the balance equations in the linear regime ($\sigma \ll \sigma_L$) of the finite membrane with large size ($L \gg L_*$). The numerical coefficient in Eq. (93) depends on microscopic details of the system at the ultraviolet scale and on the precise definition of L_*. On the other hand, the PR ν is not sensitive to the material-dependent (ultraviolet) physics and is universal in this sense. However, ν does depend on BC, as we discuss in detail below. Furthermore, if one considers a sample of an arbitrary aspect ratio, this will also influence ν. For definiteness, we focus on a square geometry of the sample below.

Before turning to the analysis of the PRs for various BCs, we notice that other elastic coefficients are also size-dependent and are related to Y_L and ν by conventional equations of the elasticity theory. In particular, the bulk and uniaxial moduli are proportional to Y_L:

$$B = \frac{Y_L}{2(1-\nu)}, \quad C_{11} = \frac{Y_L}{(1-\nu^2)}. \tag{94}$$

We emphasize again that Eqs. (91)–(94) are valid for arbitrary BC independently from the microscopic model on the ultraviolet scale. All the information on the nonuniversal (material-

dependent) ultraviolet physics is contained in the parameters Y_0 and L_* in Eq. (93).

To calculate ν in a controllable way, we consider the limit of $d_c \to \infty$, i.e., $\eta \to 0$. Naively, one could attempt to get the result by introducing an infrared cutoff $q_{\text{in}} \sim 1/L$ in the integral in Eq. (77). Neglecting σ_φ in the denominator of the integrand in Eqs. (77), we would then find that the main contribution to the integrals comes then from the lower limit q_{in}, yielding $\nu = -1/3$ independently of the exact value q_{in}. Analyzing this naive calculation, we observe that the value $1/3$ can be traced back to the ratio of two angular averages, $-\nu = \langle n_x^2 n_y^2 \rangle_\varphi / \langle n_x^4 \rangle_\varphi = 1/3$. The origin of this value is exactly the same as that of the value $\nu^{\text{diff}} = -1/3$ in the regime of nonlinear universal elasticity $\sigma_L \ll \sigma \ll \sigma_*$; see Eq. (69). One might thus come to a conclusion that the result $-1/3$ remains valid for the differential PR of the $\eta \to 0$ problem also for $\sigma \ll \sigma_L$. However, this conclusion is incorrect. Contrary to the regime $\sigma \gg \sigma_L$ [in which Eq. (69) holds], the replacement of summation by integration in the regime $\sigma \ll \sigma_L$ is not justified.

We use Eq. (47), where $\Pi_{\alpha\beta}$ are given by the diagram in Fig. 4(a) (which is the dominant contribution in the limit $\eta \to 0$). Taking into account the discreteness of momenta in course of evaluation of $\Pi_{\alpha\beta}$, we find

$$\nu = \nu^{\text{diff}} \simeq -\frac{\Pi_{xy}}{\Pi_{xx}} = -\frac{\sum_{\mathbf{q}} \frac{q_x^2 q_y^2}{q^8}}{\sum_{\mathbf{q}} \frac{q_x^4}{q^8}}. \tag{95}$$

To define unambiguously the sums in the numerator and denominator of Eq. (95), one has to specify the BCs. For the simplest case of periodic BCs, $h(x + L, y) = h(x, y + L) = h(x, y)$, quantized wave vectors are given by $q_x = 2\pi n/L, q_y = 2\pi m/L$. The point $n = m = 0$ should be excluded from summation both in the numerator and denominator of Eq. (95). We obtain

$$\nu_{\text{per}} = -\frac{4 \sum_{n=1}^{\infty} \sum_{m=1}^{\infty} \frac{n^2 m^2}{(n^2+m^2)^4}}{4 \sum_{n=1}^{\infty} \sum_{m=1}^{\infty} \frac{n^4}{(n^2+m^2)^4} + 2 \sum_{n=1}^{\infty} \frac{n^4}{(n^2)^4}} = -0.135. \tag{96}$$

This result can be straightforwardly generalized to the cases of free and zero BCs, $\partial_x h = \partial_y h = 0$ and $h = 0$, respectively:

$$\nu_{\text{free}} = -\frac{\sum_{n=1}^{\infty} \sum_{m=1}^{\infty} \frac{n^2 m^2}{(n^2+m^2)^4}}{\sum_{n=1}^{\infty} \sum_{m=1}^{\infty} \frac{n^4}{(n^2+m^2)^4} + \sum_{n=1}^{\infty} \frac{n^4}{(n^2)^4}} = -0.075 \tag{97}$$

and

$$\nu_{\text{zero}} = -\frac{\sum_{n=1}^{\infty} \sum_{m=1}^{\infty} \frac{n^2 m^2}{(n^2+m^2)^4}}{\sum_{n=1}^{\infty} \sum_{m=1}^{\infty} \frac{n^4}{(n^2+m^2)^4}} = -0.735. \tag{98}$$

Inspecting Eqs. (96)–(98), we see that ν in the linear-response regime $\sigma \ll \sigma_L$ can change dramatically (by an order of magnitude) depending on BCs. Another interesting observation is that, for some types of BCs, the differential PR is a nonmonotonic function of the stress. Indeed, comparing Eqs. (96)–(98) with Eq. (74), we see that this is the case for the periodic and free BCs, because $|\nu_{\text{per}}| < 1/3$ and $|\nu_{\text{free}}| < 1/3$. Such a situation is shown as BC 1 in Fig. 1. On the other hand, for zero BCs, $|\nu_{\text{zero}}| > 1/3$ and ν^{diff} monotonically grows with increasing σ, as shown by the BC 2 curve in Fig. 1. We remind

the reader that the values (96)–(98) are valid in the $\eta \to 0$ limit. In the case of a finite η (e.g., for a physical situation of $d_c = 1$ with $\eta \simeq 0.7$), the numerical values will be different. However, the strong variation of ν with BC will definitely persist. Furthermore, it is highly plausible that the dependence of ν^{diff} on σ will remain nonmonotonic for some BCs.

B. Fluctuations of strain and stress

Here we estimate fluctuations of the strain and stress of a finite-size system. First, we notice that for fixed configuration of out-of-plane deformation field, $\mathbf{h} = \mathbf{h}(\mathbf{r})$, the stresses σ_x and σ_y are given by Eq. (8) with only spatial averaging but without Gibbs averaging: $K_\alpha \to K_\alpha^0$; cf. Eqs. (9) and (A2). Then, we express deformations, $\varepsilon_\alpha = (\xi_\alpha^2 - \xi_0^2)/2 \approx \xi_\alpha - 1$ (neglecting the difference between ξ_0 and unity) as

$$\varepsilon_\alpha = -\frac{K_\alpha^0}{2} + \hat{M}_{\alpha\beta}^{-1}\sigma_\beta. \tag{99}$$

In the universal region, $L \gg L_*$, one can neglect the second term in Eq. (99), which yields for the distribution function of strain

$$f_\alpha(\varepsilon_\alpha) = \langle \delta(\varepsilon_\alpha + \overline{(\partial_\alpha \mathbf{h})^2}/2)\rangle. \tag{100}$$

Here $\langle \ldots \rangle$ is the Gibbs averaging for fixed σ_x and σ_y, which is taken with the functional

$$E = \frac{1}{2}\sum_{\mathbf{q}}\left(\sigma_\alpha q_\alpha^2 + \varkappa_q q^4\right)|\mathbf{h_q}|^2, \tag{101}$$

which corresponds to the approximation (58) for the Green's functions. Performing this averaging, we find

$$f_\alpha(\varepsilon_\alpha) = \int \frac{dz}{2\pi} e^{iz\varepsilon_\alpha}$$
$$\times \prod_{\mathbf{q}}\left(\frac{\varkappa_q q^4 + \sum_\beta \sigma_\beta q_\beta^2}{-izTq_\alpha^2/L^2 + \varkappa_q q^4 + \sum_\beta \sigma_\beta q_\beta^2}\right)^{d_c/2}. \tag{102}$$

Here we take into account only fluctuations of deformations caused by out-of-plane modes. One can check that the effect of in-plane modes is parametrically smaller provided that L is much larger than $\sqrt{\varkappa/\mu}$. The latter scale is on the order of the lattice constant and can be considered as an ultraviolet cutoff of the theory [74]. Hence, contribution of in-plane modes can be safely neglected.

The integrand in Eq. (102) shows a simple pole structure as a function of z thus allowing for simple analytical calculations of the moments of the deformation distribution. Evidently, $\int f_\alpha(\varepsilon_\alpha)\,d\varepsilon_\alpha = 1$. Calculating next $\langle \varepsilon_\alpha \rangle = \int f_\alpha(\varepsilon_\alpha)\varepsilon_\alpha d\varepsilon_\alpha$, we recover Eq. (11) with the Green's function $G_{\mathbf{q}} = T/(\varkappa_q q^4 + \sum_\beta \sigma_\beta q_\beta^2)$. A direct calculation of the fluctuation amplitude by using Eq. (102) yields

$$\Delta\varepsilon = \sqrt{\langle(\varepsilon_\alpha - \langle\varepsilon_\alpha\rangle)^2\rangle} = \sqrt{\frac{d_c T^2}{2L^4}\sum_{\mathbf{q}}\frac{q_\alpha^4}{\left(\varkappa_q q^4 + \sum_\beta \sigma_\beta q_\beta^2\right)^2}}, \tag{103}$$

thus leading to the the following result:

$$\Delta\varepsilon^2 \sim d_c \begin{cases} (T/\varkappa_{1/L})^2, & \text{for } \sigma \ll \sigma_L, \\ (T^2/\varkappa_{\tilde{q}_\sigma}\varkappa_{1/L})(\sigma_L/\sigma), & \text{for } \sigma \gg \sigma_L. \end{cases} \tag{104}$$

For simplicity, in Eq. (104) we considered isotropic case $\sigma_x = \sigma_y = \sigma$. Hence, fluctuations are suppressed for $\sigma \gg \sigma_L$ and become independent on σ for $\sigma \ll \sigma_L$.

In the limit $d_c \gg 1$, the distribution of strain f_α represents a Gaussian peak centered at $\langle\varepsilon_\alpha\rangle$ with a width given by Eq. (103). On the other hand, for $d_c \sim 1$, the distribution function f_α becomes essentially asymmetric at $\sigma \ll \sigma_L$.

Equation (104) yields fluctuation of strain ε at fixed stress σ. It can be used to determine fluctuations of σ at fixed strain. The result reads

$$\Delta\sigma \sim \frac{\Delta\varepsilon}{|\partial\langle(\nabla\mathbf{h})^2\rangle/\partial\sigma|} \sim \frac{\Delta\varepsilon}{|\partial\langle\varepsilon\rangle/\partial\sigma|}$$
$$\sim \frac{1}{\sqrt{d_c}}\begin{cases} \sigma_L, & \text{for } \sigma \ll \sigma_L, \\ \sqrt{(\varkappa_{\tilde{q}_\sigma}/\varkappa_{1/L})}\sqrt{\sigma_L\sigma}, & \text{for } \sigma \gg \sigma_L. \end{cases} \tag{105}$$

The factor $1/\sqrt{d_c}$ suppressing the fluctuations in the limit $d_c \to \infty$ originates from the self-averaging of the fluctuations for a large number of out-of-plane modes. As follows from Eq. (105), the strain fluctuations become much larger than the average in the linear-response regime $\sigma \ll \sigma_L$:

$$\Delta\sigma \gg \langle\sigma\rangle = \sigma \quad \text{for } \sigma \ll \sigma_L. \tag{106}$$

This means that in order to obtain correct values of thermodynamic averages in this regime out of numerical simulations, one should exert particular care to perform averaging over a sufficiently large statistical ensemble.

VI. CROSSOVER TO NONUNIVERSAL BEHAVIOR WITH DECREASING SYSTEM SIZE

Up to now we focused on the regime of large system sizes, $L \gg L_*$. Let us now analyze a crossover from this regime to that of relatively small systems, $L \lesssim L_*$. Expressing the anomalous deformation in the form

$$\frac{Y_0 \delta K_\beta}{2\sigma} = F_\beta(\sigma), \tag{107}$$

we rewrite PR as follows [see Eq. (29)]:

$$\nu = \frac{\nu_0 - F_y(\sigma)}{1 + F_x(\sigma)}. \tag{108}$$

We consider first the behavior of $\nu = \nu_L(\sigma)$ as a function of L exactly at $\sigma = 0$. Scaling properties of F_β can be understood within the approximation (58):

$$F_\beta(\sigma) = \frac{d_c T Y_0}{2L^2}\sum_{\mathbf{q}}\frac{q_\beta^2 q_x^2}{\varkappa_q q^4 (\varkappa_q q^4 + \sigma q_x^2)}. \tag{109}$$

Evaluating the sum over momenta, we find

$$F_\beta(0) \sim \begin{cases} (L/L_*)^{2-2\eta}, & L \gg L_*, \\ (L/L_*)^2, & L \ll L_*, \end{cases} \tag{110}$$

which yields the following result for the PR:

$$\nu_L(0) \approx \begin{cases} \nu_\infty(0) + A_3 (L_*/L)^{2-2\eta}, & L \gg L_*, \\ \nu_0 - A_4 (L/L_*)^2, & L \ll L_*. \end{cases} \quad (111)$$

Here $A_3 \sim 1$ and $A_4 \sim 1$ are positive numerical coefficients, while $\nu_\infty(0)$ is the PR for $\sigma = 0$ and $L = \infty$, with the limit $\sigma = 0$ taken first.

Equation (111) is general and valid for arbitrary dimensionality d_c (i.e., arbitrary η). It is in agreement with Ref. [33]. We see that with decreasing L, the PR increases from a negative value $\nu_\infty(0)$ to the positive value ν_0 prescribed by the conventional elasticity theory. The value of $\nu_\infty(0)$ depends on η and on BCs. For $\eta \to 0$, it is given by Eqs. (96)–(98) for three types of BCs. Equation (111) holds also for a disordered membrane, with a replacement $\eta \to \eta_{\mathrm{dis}} \simeq \eta/4$; see Sec. VII below.

Let us now analyze what happens at small but finite stress, $\sigma \ll \sigma_L$, assuming an arbitrary relation between L and L_*. This can be done in a controllable way in the limit $\eta \to 0$. In this limit, expression (109) becomes exact. As we demonstrated in the previous section, the behavior of the PR at small stress depends on BCs. For simplicity, we restrict ourselves to the analysis of the absolute PR of a membrane with periodic BCs. Then

$$-\nu_\infty(0) = F_y(0)/F_x(0) = -\nu_{\mathrm{per}}$$

[see Eq. (96)]. Expanding F_x and F_y over σ up to the first order and substituting these expansions into denominator and numerator of Eq. (108), we obtain

$$\nu \approx \frac{\nu_0 + \nu_{\mathrm{per}} F_0 + \tilde{\nu}_{\mathrm{per}} \sigma F_1}{1 + F_0 + \sigma F_1}. \quad (112)$$

Here $F_0 = F_x(0)$, $F_1 = (dF_x/d\sigma)_{\sigma=0}$, and

$$\tilde{\nu}_{\mathrm{per}} = -\left(\frac{dF_y/d\sigma}{dF_x/d\sigma} \right)_{\sigma=0}$$

$$= \frac{2 \sum_{n=1}^{n=\infty} \sum_{m=1}^{m=\infty} \frac{m^2 n^4}{(n^2+m^2)^6}}{2 \sum_{n=1}^{n=\infty} \sum_{m=1}^{m=\infty} \frac{n^6}{(n^2+m^2)^6} + \sum_{n=1}^{n=\infty} \frac{1}{n^6}} \simeq -0.03. \quad (113)$$

The sum in the last equation is obtained exactly in full analogy with Eq. (96). It is worth mentioning that the absolute value of $\tilde{\nu}_{\mathrm{per}}$ is numerically an order of magnitude smaller than a naive result,

$$\tilde{\nu}_{\mathrm{per}}^{\mathrm{continous}} = -\frac{\langle n_x^4 n_y^2 \rangle_\varphi}{\langle n_x^6 \rangle_\varphi} = -\frac{1}{5},$$

that one would get by using a continuous approximation, with all sums in Eq. (113) replaced with the integrals. Equation (112) implies that at a certain value of L/L_* the derivative $(\partial \nu / \partial \sigma)_{\sigma \to 0}$ changes sign. Differentiating Eq. (112) over σ, we find that the value of the PR at this point is given exactly by $\tilde{\nu}_{\mathrm{per}}$:

$$\left(\frac{d\nu}{d\sigma} \right)_{\sigma=0} = 0 \quad \text{for} \quad \nu = \tilde{\nu}_{\mathrm{per}}. \quad (114)$$

Thus, for periodic BCs, the dependence $\nu(\sigma)$ evolves from a nonmonotonic to a monotonic one with lowering L/L_*, as illustrated in Fig. 5. In Fig. 6 we show how the dependence of ν on the system size L evolves with increasing stress σ.
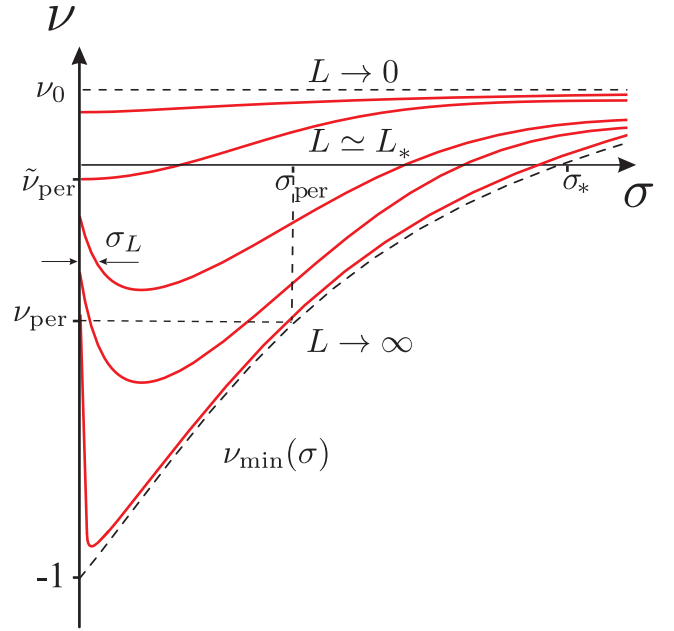
FIG. 5. Evolution of the stress dependence of absolute PR $\nu_L(\sigma)$ with changing system size L for periodic boundary conditions. With increasing ratio L/L_* the curve $\nu(\sigma)$ moves downwards. Lower dashed line: $L/L_* \to \infty$; upper dashed line: $L/L_* \to 0$. The value σ_{per} is defined by condition $\nu_{\mathrm{min}}(\sigma_{\mathrm{per}}) = \nu_{\mathrm{per}}$. For $\eta \to 0$, the limiting value $\nu_{\mathrm{min}}(0)$ is equal to -1, as shown in the plot. The values of ν_{per} and $\tilde{\nu}_{\mathrm{per}}$ are then given by Eqs. (96) and (113), respectively. For a generic case (including the physical case of $d_c = 1$ with $\eta \approx 0.7$–0.8) the numerical values are different but the qualitative behavior is expected to be the same.

VII. DISORDERED MEMBRANE

In this section, we discuss briefly a generalization of the results of this paper on the disordered case. A more detailed analysis will be presented elsewhere. Physically, the clean and disordered cases are quite similar. As was recently demonstrated [72], the bending rigidity of a strongly disordered membrane scales in a power-law way in a wide interval of q: $\varkappa_q \propto 1/q^{\eta_{\mathrm{dis}}}$. For small d_c, the critical index of the disordered problem is related to that of a clean system via $\eta_{\mathrm{dis}} \simeq \eta/4$. The power-law dependence of the effective isotropic stiffness, (23), is also valid for strongly disordered membrane with the critical index $\alpha^{\mathrm{dis}} = \eta_{\mathrm{dis}}/(2 - \eta_{\mathrm{dis}}) \simeq \eta/(8 - \eta)$. Hence, the clean and strongly disordered systems belong to different universality classes, i.e., exhibit power-law scaling of κ_q characterized by different exponents, and are thus characterized by distinct values of ν.

For a given value of η (determined by the spatial dimension d_c) and the same BCs, we expect the PR of a large ($L \gg L_*$) disordered membrane to be lower than that for a clean membrane: $\nu_{\mathrm{dis}}(\sigma) < \nu_{\mathrm{clean}}(\sigma)$; see Fig. 7. Indeed, as has been demonstrated above, the PR tends to a universal curve ν_{min} with decreasing η. Since the effective η for a disordered membrane is smaller than for a clean one, $\eta_{\mathrm{dis}} \simeq \eta/4 < \eta$, the value of PR should be closer to this universal curve. This conclusion is in agreement with the numerical simulations that predicted a stronger auxetic behavior (i.e., more negative values of PR) for artificially disordered membranes [22–24]; see Sec. I.
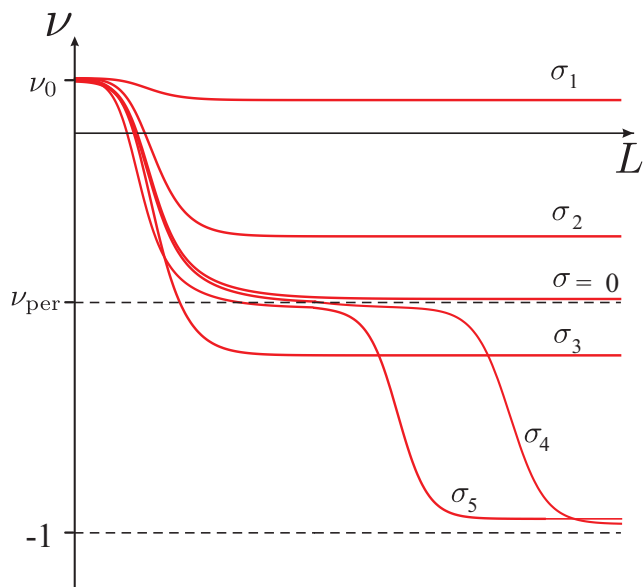
FIG. 6. Length dependence of the absolute Poisson ratio for periodic BCs and different values of the applied stress. The curves correspond to the following: large stress, $\sigma_1 \gg \sigma_*$; intermediate stress, $\sigma_2 \gtrsim \sigma_{\text{per}} \sim \sigma_*$ (with σ_{per} as defined in Fig. 5); relatively small stress, $\sigma_3 \lesssim \sigma_{\text{per}}$; low stresses, σ_4 and σ_5 (with $\sigma_4 < \sigma_5$); and zero stress, $\sigma = 0$. For large stress σ_1, the PR is close to ν_0 within the whole interval of L. The curves corresponding to $\sigma \ll \sigma_*$ ($\sigma = \sigma_4$ and $\sigma = \sigma_5$) show a well developed intermediate plateau at $\nu = \nu_{\text{per}}$ and eventually saturate at $\nu = \nu_{\text{min}}(\sigma)$ which approaches $\nu_{\text{min}}(0)$. For $\eta \to 0$, the value $\nu_{\text{min}}(0)$ is equal to -1, as shown in the plot. The value of ν_{per} is then given by Eqs (96). For a generic case, the numerical values are different but the qualitative behavior is expected to be the same.
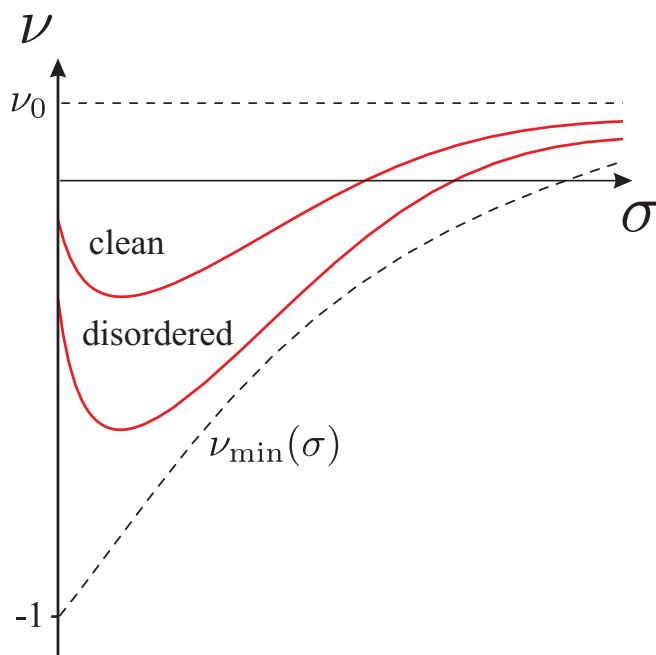
FIG. 7. Schematic plot of the stress dependence of PR of a strongly disordered membrane as compared to a clean membrane with the same value of η.
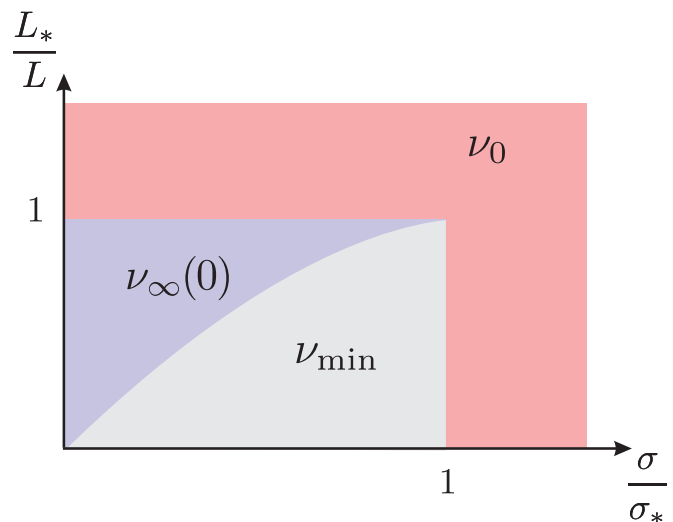
FIG. 8. Regimes of asymptotic behavior of Poisson ratio in the parameter plane spanned by the stress and the system size. Crossovers between respective regimes take place around the lines $\sigma/\sigma_* \sim 1$, $L_*/L \sim 1$, and $\sigma/\sigma_* \sim (L_*/L)^{2-\eta}$.

An important hallmark of the disordered case is mesoscopic fluctuations of the observables, in particular, of PR. These fluctuations become particularly prominent in the low-stress regime, $\sigma \ll \sigma_L$, when all the infrared divergencies are regularized by the system size, so that no self-averaging occurs. In particular, the mesoscopic fluctuations of PR at $\sigma \ll \sigma_L$ should be of order unity.

VIII. SUMMARY AND DISCUSSION

To conclude, we have studied the system-size and stress dependence of the Poisson ratio of graphene (or, more generally, of a 2D membrane). The "phase diagram" of various asymptotic regimes of the behavior of PR is presented in Fig. 8. Our analysis, including the phase diagram, scaling, universality, as well as importance to distinguish between the absolute and differential PRs, is valid for any spatial dimensionality d_c, including the physical case $d_c = 1$. It has been supplemented by an evaluation of the PR in the limit of high dimensionality of the embedding space, $d_c \gg 1$, i.e., $\eta \ll 1$.

Our predictions for a large system, $L \gg L_*$, are schematically summarized in Fig. 1. The red and blue curves represent the stress dependence of the absolute PR, ν, and the differential PR, ν^{diff}, respectively. One can observe the two characteristic scales of the stress, σ_* and σ_L, which subdivide the σ axis into three distinct regimes.

For high stress, $\sigma \gg \sigma_*$, nonlinear effect are suppressed, the membrane obeys the conventional linear Hooke's law, and the PR (both absolute and differential) is given by its bare (material-dependent) value ν_0,

$$\nu_0 = \frac{\lambda_0}{2\mu_0 + \lambda_0}. \tag{115}$$

For graphene $\nu_0 \simeq 0.1$.

For low tensions, $\sigma \ll \sigma_L$, elastic properties of the membrane are dominated by finite-size effects. In this case, the

membrane shows linear response with respect to external forces, so that the absolute and differential PRs coincide: $\nu = \nu^{\mathrm{diff}} = \nu_\infty(0)$. Here $\nu_\infty(0)$ stands for the following order of limits: *first* one sends σ to zero and *next* $L \to \infty$ (in fact, $L \gg L_*$ is sufficient). An important prediction is a strong dependence of $\nu_\infty(0)$ on boundary conditions. For three types of BCs—periodic, free, and zero—we find that $\nu_\infty(0)$ is given, in the limit $\eta \to 0$, by $\nu_{\mathrm{per}} = -0.135$, $\nu_{\mathrm{free}} = -0.075$, and $\nu_{\mathrm{zero}} = -0.735$, respectively. In this regime, the value of ν is universal in the sense that it does not depend on material parameters. It depends, however, on spatial dimensionality d_c (i.e., on η) and on BCs. These results for the low-tension regime are qualitatively consistent with numerical simulations of membranes in Refs. [34–36] which yielded negative values of PR and indicated the importance of boundary conditions.

In the intermediate interval $\sigma_L \ll \sigma \ll \sigma_*$ the membrane falls into the universal nonlinear regime, where the difference between the absolute and differential PRs is essential, $\nu \neq \nu^{\mathrm{diff}}$. For $\eta \to 0$, both absolute and differential PRs can be calculated analytically in a controllable way:

$$\nu \to -1 + (1 + C_\Sigma)\eta + O(\eta^2),$$
$$\nu^{\mathrm{diff}} \to -1/3 + 0.008\eta + O(\eta^2), \tag{116}$$

where C_Σ is a numerical coefficient. It is worth stressing again that the absolute and differential PRs in this regime have a high degree of universality: they depend only on the spatial dimensionality d_c (or, equivalently, on η). We also notice that the numerical coefficient in the first-order expansion of ν_{diff} with respect to η is very small, so that in the physical case, $d_c = 1$, the differential PR may be expected to be relatively close to $-1/3$. However, we cannot exclude at this stage a possibility that higher-order corrections are numerically larger. Therefore, high-precision numerical simulations would be highly desirable to check the above expectation.

An interesting consequence of these findings is a non-monotonic dependence of the PR on stress. As seen from Fig. 1, the absolute PR at small η is nonmonotonic for any BC, because $\nu_\infty(0) > -1$ for all BCs. On the other hand, the differential PR is nonmonotonic for periodic and free BCs (since $\nu_{\mathrm{per}} > -1/3$ and $\nu_{\mathrm{free}} > -1/3$), and monotonic for zero BC (since $\nu_{\mathrm{zero}} < -1/3$).

We have further discussed the evolution of the above results with decreasing system size, when the system evolves towards the nonuniversal regime, $L < L_*$. While the general tendency is quite simple—both ν and ν^{diff} tend to the nonuniversal value ν_0—dependencies of PR on σ for different L and on L for different σ show interesting features, as illustrated in Figs. 5 and 6. In particular, the dependence of ν on L for a fixed stress demonstrates a wide plateau for sufficiently low σ.

The results described above are applicable to generic membranes, including freestanding graphene. Qualitatively, different regimes of behavior of the PR (schematically presented in Fig. 1) are better visualized if one uses the logarithmic scale for stress. In Fig. 9, we present in this way the results for the absolute PR using the graphene parameters. Estimates have been made for the room temperature in a very wide range of sample sizes: from 10 Å to 1 cm. We used cyclic boundary conditions. The value of σ_* was estimated as $\sigma_* = 0.1$ N/m [73] and the Ginzburg length as $L_* = 50\,\text{Å}$ [72]. The curves
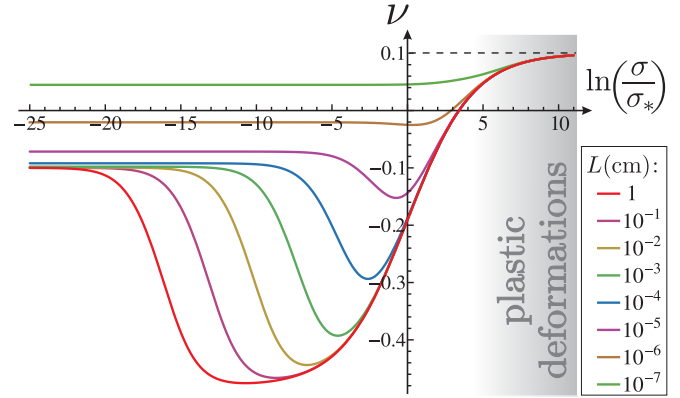
FIG. 9. Stress dependence of the absolute Poisson ratio of free-standing graphene at $T = 300$ K in samples of different size (see text for details). Region marked by gray color corresponds to very large strains, $\sigma > 50$ N/m, where a physical graphene membrane is affected by plastic deformations not included in our theory.

have been obtained by interpolating between scaling dependencies that describe different regions. The region of large stress corresponding to plastic deformations (not included in our theory) is marked by gray color. The border between elastic and plastic deformations, σ_{plast}, is estimated as follows. Plasticity comes into play at deformations on the order of 20% [77]. Since the Young modulus of graphene equals 340 N/m, we estimate $\sigma_{\mathrm{plast}} \simeq 50$ N/m, thus obtaining $\ln(\sigma_{\mathrm{plast}}/\sigma_*) \simeq 6$. It is seen from Fig. 9 that in order to observe all three regimes ("mesoscopic," universal, and conventional elasticity) one has to pass a rather wide interval of stresses. It is also worth noting that the region of conventional elasticity has a strong overlap with the plasticity region. In other words, the elasticity of graphene is mainly anomalous.

We have also discussed qualitatively the case of a disordered membrane. The key difference is that the effective η for a disordered membrane is smaller than for clean one, $\nu_{\mathrm{dis}} \simeq \nu/4 < \eta$. Since the dependence ν on σ tends to $\nu_{\mathrm{min}}(\sigma)$ with decreasing η (for $L \to \infty$), the value of the PR for a disordered membrane should be closer to the universal curve $\nu(\sigma)$; see Fig. 7. A hallmark of a disordered membrane is strong mesoscopic (sample-to-sample) fluctuations of PR in the linear-response regime, $\sigma \ll \sigma_L$. Our conclusions are in agreement with numerical simulations which found a more pronounced auxetic behavior for artificially disordered graphene membranes [22–24]. Furthermore, Fig. 3 of Ref. [22] shows a strongly nonmonotonic behavior of PR as a function of applied stress for disordered graphene, in full consistency with our Fig. 1. On the other hand, for the case of clean graphene, an initial reduction of PR for the smallest stresses was observed in Ref. [22] (see upper panel of their Fig. 3). The reason for this was likely an insufficient system size; see Fig. 5 of our work. The disorder reduces the Ginzburg length L_*, thus allowing one to probe better the universal regime $L \gg L_*$ for a given system size L.

Our work paves the way for detailed studies of PR and related properties of graphene and other 2D membranes. Since the physical situation of $d_c = 1$ ($\eta \approx 0.7$–0.8) does not belong to the regime $d_c \to \infty$ ($\eta \to 0$) where our

analytical calculations of the asymptotic values of PR are fully controllable, systematic numerical simulations would be of great interest. Identification of the three regimes (see Figs. 1 and 8) in such simulations is expected to be a feasible although rather challenging task. A more ambitious goal is a sufficiently precise determination of the asymptotic values of the absolute and differential PRs in the nonlinear universal regime, as well as of PRs in the linear-response regime for various BCs.

We hope that our work will also stimulate further experimental activities on nanomechanics of clean and disordered graphene (and related 2D materials), both in the linear and nonlinear regime with respect to the applied stress. In particular, an experimental realization of regimes of auxetic behavior identified and analyzed in our work would be of great interest.

APPENDIX: DERIVATION OF THE FREE ENERGY AND BALANCE EQUATIONS OF THE ANISOTROPICALLY LOADED MEMBRANE

In this appendix, we present a derivation of Eqs. (8) and (10) of the main text as well their generalization to the case of a membrane of arbitrary dimensionality D.

We write the energy functional (5) in terms of the components of the stretching vector ξ_x, ξ_y [see Eq. (7)], in-plane fluctuations $\mathbf{u}$, and out-of-plane fluctuations $\mathbf{h}$:

$$E = L^2 \sum_{\alpha\beta} \left[\frac{\mu_0}{4} \delta_{\alpha\beta} + \frac{\lambda_0}{8} \right] \left[s_\alpha s_\beta - K_\alpha^0 K_\beta^0 \right] + E_0(\mathbf{u},\mathbf{h}),$$

(A1)

where

$$K_\alpha^0 = \overline{(\partial_\alpha \mathbf{h})^2} = \int \frac{d^2 x}{L^2} (\partial_\alpha \mathbf{h})^2 \qquad (A2)$$

[here $\overline{(\cdots)}$ stands for the spatial averaging],

$$s_\alpha = \xi_\alpha^2 - 1 + K_\alpha^0, \qquad (A3)$$

and

$$E_0(\mathbf{u},\mathbf{h}) = \int d^2 x \left\{ \frac{\varkappa}{2} (\Delta \mathbf{h})^2 + \mu_0 u_{ij}^2 + \frac{\lambda_0}{2} u_{ii}^2 \right\}. \qquad (A4)$$

Here

$$u_{\alpha\beta} = \left(\xi_\beta \partial_\alpha u_\beta + \xi_\alpha \partial_\beta u_\alpha + \partial_\alpha \mathbf{h} \partial_\beta \mathbf{h} \right)/2$$

is the strain tensor (the rule of summation over repeated indices does not apply). For small deformations, one can put $\xi_x = \xi_y = 1$ in the strain tensor, so that $E_0(\mathbf{u},\mathbf{h})$ coincides with the conventional expression for elastic energy of a nearly flat membrane.

The next step is to calculate free energy corresponding to energy functional Eq. (A1):

$$F = -T \ln \left(\int \{d\mathbf{u} d\mathbf{h}\} e^{-E/T} \right). \qquad (A5)$$

This can be done in an analogy with isotropic case (see technical details in the Supplemental Material of Ref. [73]). We decouple the term $s_\alpha s_\beta$ with the use of the auxiliary fields χ_α:

$$\exp\left[-\frac{L^2}{4T} (\mu_0 \delta_{\alpha\beta} + \lambda_0/2) s_\alpha s_\beta \right] \qquad (A6)$$

$$\propto \int d\chi_\alpha \exp\left\{ \frac{L^2}{2T} \sum_{\alpha\beta} \left[\delta_{\alpha\beta} \left(i s_\alpha \chi_\beta - \frac{\chi_\alpha \chi_\beta}{2\mu} \right) \right. \right.$$

$$\left. \left. + \frac{\lambda_0 \chi_\alpha \chi_\beta}{4\mu_0(\mu_0 + \lambda_0)} \right] \right\}. \qquad (A7)$$

Evaluating the integrals over the in-plane modes $\mathbf{u}$ and out-of plane modes $\mathbf{h}$, we find

$$\Phi(\sigma,\xi) = \frac{L^2}{2} \left\{ \sum_\alpha \left[\sigma_\alpha \left(\xi_\alpha^2 - 1 \right) - \frac{\sigma_\alpha^2}{2\mu_0} \right] \right.$$

$$+ \frac{\lambda_0}{4\mu_0(\mu_0 + \lambda_0)} \left(\sum_\alpha \sigma_\alpha \right)^2 \right\}$$

$$+ \frac{T d_c}{2} \sum_\mathbf{q} \ln\left(\varkappa_q q^4 + \sum_\alpha \sigma_\alpha q_\alpha^2 \right), \qquad (A8)$$

where $\sigma_\alpha = -i\chi_\alpha^{(0)}$ and $\chi_\alpha^{(0)}$ correspond to stationary phase condition for integral over $d\chi_\alpha$. This condition, $\partial \Phi(\sigma,\xi)/\partial \sigma_\alpha = 0$, yields the balance equations for a 2D membrane as presented in Eqs. (8) and (10) of the main text. Inserting the corresponding equilibrium values $\sigma_\alpha(\xi_x,\xi_y)$ in the functional $\Phi(\sigma_x,\sigma_y,\xi_x,\xi_y)$, we find the free energy $F(\xi_x,\xi_y)$ as a function of the stretching vector (ξ_x,ξ_y). The stationary-point value $\sigma_\alpha(\xi_x,\xi_y)$ determines the physical stress. Indeed, it is easy to check that $\sigma_\alpha = (1/L^2\xi_\alpha)\partial F/\partial \xi_\alpha$ (no summation over α); i.e., σ is conjugate to the strain ξ. Deep in the flat phase, $\xi_\alpha \approx 1$, and we find

$$\sigma_\alpha = \frac{1}{L^2} \frac{\partial F}{\partial \xi_\alpha}. \qquad (A9)$$

These results can be straightforwardly generalized to the case of a membrane of an arbitrary dimensionality D. We assume that the membrane is loaded in a certain direction by uniaxial stress, with equal deformations in other $D-1$ directions. First, we neglect anomalous deformations. We get then the following matrix of elastic constants of a membrane:

$$\hat{M} = \begin{pmatrix} 2\mu_0 + \lambda_0 & \lambda_0 \\ \lambda_0(D-1) & 2\mu_0 + \lambda_0(D-1) \end{pmatrix}, \qquad (A10)$$

which generalizes Eq. (10) of the main text. Using a standard definition of elastic moduli, we thus obtain

$$B = \lambda_0 + \frac{2\mu_0}{D}, \qquad (A11)$$

$$Y_0 = \frac{2\mu_0(2\mu_0 + D\lambda_0)}{2\mu_0 + \lambda_0(D-1)}, \qquad (A12)$$

$$C_{11} = 2\mu_0 + \lambda_0, \tag{A13}$$

$$\nu_0 = \frac{\lambda_0}{2\mu_0 + \lambda_0(D-1)}. \tag{A14}$$

These equations can be extended to include anomalous deformations. In particular, the differential PR ν^{diff} is expressed in terms of the renormalized elastic parameters μ^{diff} and λ^{diff} by a formula that has the same form as Eq. (A14). In the universal nonlinear regime (where the anomalous deformations dominate), and in the limit $d_c \to \infty$, the results of Ref. [30] apply,

yielding the invariant manifold of the Lamé coefficients,

$$\lambda^{\text{diff}} = -\frac{2\mu^{\text{diff}}}{D+2}, \quad d_c = \infty; \tag{A15}$$

cf. Eq. (46) for $\Pi_+ = \Pi_-$. Hence, we get

$$\nu^{\text{diff}} = -\tfrac{1}{3} \quad \text{for} \quad d_c = \infty. \tag{A16}$$

Thus, for $d_c \to \infty$, the value $-1/3$ of the differential PR in the nonlinear universal regime is independent of the membrane dimensionality D. As explained in the main text for the case of 2D membranes, this value gets modified when one considers a finite dimensionality d_c.

[1] K. E. Evans, M. A. Nkansah, I. J. Hutchinson, and S. C. Rogers, Nature (London) **353**, 124 (1991).

[2] A. E. H. Love, *A Treatise on the Mathematical Theory of Elasticity*, 4th ed. (Dover, New York, 1944), p. 163.

[3] R. Lakes, Science **235**, 1038 (1987).

[4] J.-W. Jiang, S. Y. Kim, and H. S. Park, Appl. Phys. Rev. **3**, 041101 (2016).

[5] K. S. Novoselov, A. K. Geim, S. V. Morozov, D. Jiang, Y. Zhang, S. V. Dubonos, I. V. Grigorieva, and A. A. Firsov, Science **306**, 666 (2004).

[6] K. S. Novoselov, A. K. Geim, S. V. Morozov, D. Jiang, M. I. Katsnelson, I. V. Grigorieva, S. V. Dubonos, and A. A. Firsov, Nature (London) **438**, 197 (2005).

[7] Y. Zhang, Y.-W. Tan, H. L. Stormer, and P. Kim, Nature (London) **438**, 201 (2005).

[8] A. K. Geim and K. S. Novoselov, Nat. Mater. **6**, 183 (2007).

[9] A. H. Castro Neto, F. Guinea, N. M. R. Peres, K. S. Novoselov, and A. K. Geim, Rev. Mod. Phys. **81**, 109 (2009).

[10] S. Das Sarma, S. Adam, E. H. Hwang, and E. Rossi, Rev. Mod. Phys. **83**, 407 (2011).

[11] V. N. Kotov, B. Uchoa, V. M. Pereira, F. Guinea, and A. H. Castro Neto, Rev. Mod. Phys. **84**, 1067 (2012).

[12] M. I. Katsnelson, *Graphene: Carbon in Two Dimensions* (Cambridge University Press, Cambridge, 2012).

[13] M. I. Katsnelson and A. Fasolino, Acc. Chem. Res. **46**, 97 (2013).

[14] E. L. Wolf, *Graphene: A New Paradigm in Condensed Matter and Device Physics* (Oxford University Press, Oxford, 2014).

[15] L. E. F. Foa Torres, S. Roche, and J.-C. Charlier, *Introduction to Graphene-Based Nanomaterials: From Electronic Structure to Quantum Transport* (Cambridge University Press, Cambridge, 2014).

[16] D. Nelson, T. Piran, and S. Weinberg, editors, *Statistical Mechanics of Membranes and Surfaces* (World Scientific, Singapore, 1989).

[17] G. Cao, Polymers **6**, 2404 (2014).

[18] A. Politano and G. Chiarello, Nano Res. **8**, 1847 (2015).

[19] K. V. Zakharchenko, M. I. Katsnelson, and A. Fasolino, Phys. Rev. Lett. **102**, 046808 (2009).

[20] J. H. Los, A. Fasolino, and M. I. Katsnelson, Phys. Rev. Lett. **116**, 015901 (2016).

[21] G. Gui, J. Li, and J. Zhong, Phys. Rev. B **78**, 075435 (2008).

[22] J. N. Grima, S. Winczewski, L. Mizzi, M. C. Grech, R. Cauchi, R. Gatt, D. Attard, K. W. Wojciechowski, and J. Rybicki, Adv. Mater. **27**, 1455 (2015).

[23] H. Qin, Y. Sun, J. Z. Liu, M. Lia, and Y. Liu, Nanoscale **9**, 4135 (2017).

[24] J. Wan, J.-W. Jiang, and H. S. Park, Nanoscale **9**, 4007 (2017).

[25] J.-W. Jiang, T. Chang, X. Guo, and H. S. Park, Nano Lett. **16**, 5286 (2016).

[26] Z. W. Ulissi, A. G. Rajan, and M. S. Strano, ACS Nano **10**, 7542 (2016).

[27] J.-W. Jiang and H. S. Park, Nano Lett. **16**, 2657 (2016).

[28] Y. Wu, N. Yi, L. Huang, T. Zhang, S. Fang, H. Chang, N. Li, J. Oh, J. A. Lee, M. Kozlov, A. C. Chipara, H. Terrones, P. Xiao, G. Long, Y. Huang, F. Zhang, L. Zhang, X. Lepro, C. Haines, M. D. Lima, N. P. Lopez, L. P. Rajukumar, A. L. Elias, S. Feng, S. J. Kim, N. T. Narayanan, P. M. Ajayan, M. Terrones, A. Aliev, P. Chu, Z. Zhang, R. H. Baughman, and Y. Chen, Nat. Commun. **6**, 6141 (2015).

[29] V. H. Ho, D. T. Ho, S.-Y. Kwon, and S. Y. Kim, Phys. Status Solidi B **253**, 1303 (2016).

[30] P. Le Doussal and L. Radzihovsky, Phys. Rev. Lett. **69**, 1209 (1992).

[31] A. Kosmrlj and D. R. Nelson, Phys. Rev. E **88**, 012136 (2013); **89**, 022126 (2014).

[32] P. Le Doussal and L. Radzihovsky, Annals Phys. (2018), doi:10.1016/j.aop.2017.08.033.

[33] A. Kosmrlj and D. R. Nelson, Phys. Rev. B **93**, 125431 (2016).

[34] Z. Zhang, H. T. Davis, and D. M. Kroll, Phys. Rev. E **53**, 1422 (1996).

[35] M. Falcioni, M. J. Bowick, E. Guitter, and G. Thorleifsson, Europhys. Lett. **38**, 67 (1997).

[36] M. Bowick, A. Cacciuto, G. Thorleifsson, and A. Travesset, Phys. Rev. Lett. **87**, 148103 (2001).

[37] Recently, numerical simulations of Ref. [31] indicated a positive PR for warped 2D membranes at zero temperature, whereas the scaling exponents were found to be in agreement with their SCSA values. The authors of Ref. [31] argued that the SCSA might be insufficient for calculating the PR.

[38] N. D. Mermin and H. Wagner, Phys. Rev. Lett. **17**, 1133 (1966); N. D. Mermin, Phys. Rev. **176**, 250 (1968).

[39] L. D. Landau and E. M. Lifshitz, *Statistical Physics*, Part 1 (Pergamon Press, Oxford, 1980).

[40] D. R. Nelson and L. Peliti, J. Phys. (Paris) **48**, 1085 (1987).

[41] Y. Kantor and D. R. Nelson, Phys. Rev. Lett. **58**, 2774 (1987); Phys. Rev. A **36**, 4020 (1987).

[42] M. Paczuski, M. Kardar, and D. R. Nelson, Phys. Rev. Lett. **60**, 2638 (1988).

[43] F. David and E. Guitter, Europhys. Lett. **5**, 709 (1988).

[44] E. Guitter, F. David, S. Leibler, and L. Peliti, Phys. Rev. Lett. **61**, 2949 (1988).

[45] J. A. Aronovitz and T. C. Lubensky, Phys. Rev. Lett. **60**, 2634 (1988).

[46] E. Guitter, F. David, S. Leibler, and L. Peliti, J. Phys. (France) **50**, 1787 (1989).

[47] J. Aronovitz, L. Golubović, and T. C. Lubensky, J. Phys. (France) **50**, 609 (1989).

[48] M. Paczuski and M. Kardar, Phys. Rev. A **39**, 6086 (1989).

[49] L. Radzihovsky and D. R. Nelson, Phys. Rev. A **44**, 3525 (1991).

[50] D. R. Nelson and L. Radzihovsky, Europhys. Lett. **16**, 79 (1991).

[51] G. Gompper and D. M. Kroll, Europhys. Lett. **15**, 783 (1991).

[52] L. Radzihovsky and P. Le Doussal, J. Phys. I (France) **2**, 599 (1992).

[53] D. C. Morse, T. C. Lubensky, and G. S. Grest, Phys. Rev. A **45**, R2151 (1992).

[54] P. Le Doussal and L. Radzihovsky, Phys. Rev. B **48**, 3548 (1993).

[55] M. J. Bowick, S. M. Catterall, M. Falcioni, G. Thorleifsson, and K. N. Anagnostopoulos, J. Phys. I (France) **6**, 1321 (1996).

[56] J. H. Los, M. I. Katsnelson, O. V. Yazyev, K. V. Zakharchenko, and A. Fasolino, Phys. Rev. B **80**, 121405(R) (2009).

[57] J.-P. Kownacki and D. Mouhanna, Phys. Rev. E **79**, 040101(R) (2009).

[58] D. Gazit, Phys. Rev. E **80**, 041117 (2009).

[59] D. Gazit, Phys. Rev. B **80**, 161406(R) (2009).

[60] F. L. Braghin and N. Hasselmann, Phys. Rev. B **82**, 035407 (2010).

[61] V. V. Lebedev and E. I. Kats, Phys. Rev. B **85**, 045416 (2012).

[62] E. I. Kats and V. V. Lebedev, Phys. Rev. B **89**, 125433 (2014).

[63] B. Amorim, R. Roldán, E. Cappelluti, A. Fasolino, F. Guinea, and M. I. Katsnelson, Phys. Rev. B **89**, 224307 (2014).

[64] E. I. Kats and V. V. Lebedev, Phys. Rev. E **91**, 032415 (2015).

[65] C. Lee, X. Wei, J. W. Kysar, and J. Hone, Science **321**, 385 (2008).

[66] D. Metten, F. Federspiel, M. Romeo, and S. Berciaud, Phys. Rev. Appl. **2**, 054008 (2014).

[67] M. K. Blees, A. W. Barnard, P. A. Rose, S. P. Roberts, K. L. McGill, P. Y. Huang, A. R. Ruyack, J. W. Kevek, B. Kobrin, D. A. Muller, and P. L. McEuen, Nature (London) **524**, 204 (2015).

[68] G. Lopez-Polin, C. Gomez-Navarro, V. Parente, F. Guinea, M. I. Katsnelson, F. Perez-Murano, and J. Gomez-Herrero, Nat. Phys. **11**, 26 (2015); G. Lopez-Polin, M. Jaafar, F. Guinea, R. Roldan, C. Gomez-Navarro, and J. Gomez-Herrero, Carbon **124**, 42 (2017).

[69] R. J. T. Nicholl, H. J. Conley, N. V. Lavrik, I. Vlassiouk, Y. S. Puzyrev, V. P. Sreenivas, S. T. Pantelides, and K. I. Bolotin, Nat. Commun. **6**, 8789 (2015).

[70] I. V. Gornyi, V. Yu. Kachorovskii, and A. D. Mirlin, Phys. Rev. B **86**, 165413 (2012).

[71] T. Zhu and E. Ertekin, Phys. Rev. B **90**, 195209 (2014); **91**, 205429 (2015).

[72] I. V. Gornyi, V. Yu. Kachorovskii, and A. D. Mirlin, Phys. Rev. B **92**, 155428 (2015).

[73] I. V. Gornyi, V. Yu. Kachorovskii, and A. D. Mirlin, 2D Mater. **4**, 011003 (2017).

[74] I. S. Burmistrov, I. V. Gornyi, V. Yu. Kachorovskii, M. I. Katsnelson, and A. D. Mirlin, Phys. Rev. B **94**, 195430 (2016).

[75] I. M. Lifshitz, Zh. Eksp. Teor. Fiz. **22**, 475 (1952).

[76] I. S. Burmistrov, I. V. Gornyi, V. Yu. Kachorovskii, and A. D. Mirlin, arXiv:1801.05053.

[77] M. Topsakal and S. Ciraci, Phys. Rev. B **81**, 024107 (2010).